

University of Nebraska - Lincoln

DigitalCommons@University of Nebraska - Lincoln

Faculty Publications from the Center for Plant
Science Innovation

Plant Science Innovation, Center for

2018

MAC3A and MAC3B, Two Core Subunits of the MOS4-Associated Complex, Positively Influence miRNA biogenesis

Shengjun Li

University of Nebraska-Lincoln, sli39@unl.edu

Kan Liu

University of Nebraska-Lincoln, kliu7@unl.edu

Bangjun Zhou

University of Nebraska-Lincoln,, bzhou3@unl.edu

Mu Li

University of Nebraska-Lincoln, mli17@unl.edu

Shuxin Zhang

Shandong Agricultural University

See next page for additional authors

Follow this and additional works at: <https://digitalcommons.unl.edu/plantscifacpub>



Part of the [Plant Biology Commons](#), [Plant Breeding and Genetics Commons](#), and the [Plant Pathology Commons](#)

Li, Shengjun; Liu, Kan; Zhou, Bangjun; Li, Mu; Zhang, Shuxin; Zeng, Lirong; Zhang, Chi; and Yu, Bin, "MAC3A and MAC3B, Two Core Subunits of the MOS4-Associated Complex, Positively Influence miRNA biogenesis" (2018). *Faculty Publications from the Center for Plant Science Innovation*. 183.
<https://digitalcommons.unl.edu/plantscifacpub/183>

This Article is brought to you for free and open access by the Plant Science Innovation, Center for at DigitalCommons@University of Nebraska - Lincoln. It has been accepted for inclusion in Faculty Publications from the Center for Plant Science Innovation by an authorized administrator of DigitalCommons@University of Nebraska - Lincoln.

Authors

Shengjun Li, Kan Liu, Bangjun Zhou, Mu Li, Shuxin Zhang, Lirong Zeng, Chi Zhang, and Bin Yu

1 **RESEARCH ARTICLE**

2
3 **MAC3A and MAC3B, Two Core Subunits of the MOS4-Associated Complex,**
4 **Positively Influence miRNA biogenesis**

5
6 **Shengjun Li^{1,2,3}, Kan Liu^{2,3}, Bangjun Zhou^{2,4}, Mu Li^{2,3}, Shuxin Zhang⁵, Lirong Zeng^{2,4}, Chi Zhang^{2,3}**
7 **and Bin Yu^{2,3*}**

8
9 ¹Qingdao Engineering Research Center of Biomass Resources and Environment, Qingdao Institute of
10 Bioenergy and Bioprocess Technology, Chinese Academy of Sciences, Qingdao 266101, China

11 ²Center for Plant Science Innovation University of Nebraska-Lincoln, Lincoln, Nebraska 68588–0666,
12 USA

13 ³School of Biological Sciences, University of Nebraska-Lincoln, Lincoln, Nebraska 68588–0118, USA

14 ⁴Department of Plant Pathology, University of Nebraska, Lincoln, NE 68583-0722

15 ⁵ State Key Laboratory of Crop Biology, College of Life Sciences, Shandong Agricultural University,
16 Taian 271018, China

17
18 *Corresponding author: byu3@unl.edu

19
20 **Short title:** MAC3A and MAC3B in miRNA biogenesis

21
22 **One-sentence summary:** The MOS4-associated complex promotes miRNA accumulation by positively
23 modulating pri-miRNA transcription, stability and processing.

24
25 The author responsible for distribution of materials integral to the findings presented in this manuscript in
26 accordance with the policy described in the Instructions for Authors (www.plantcell.org) is: Bin Yu
27 (byu3@unl.edu)

28
29 **ABSTRACT**

30 MAC3A and MAC3B are conserved U-box containing proteins in eukaryotes. They are subunits of the
31 MOS4-associated complex (MAC) that plays essential roles in plant immunity and development in
32 Arabidopsis. However, their functional mechanisms remain elusive. Here we show that *Arabidopsis*
33 *thaliana* MAC3A and MAC3B act redundantly in microRNA (miRNA) biogenesis. Lack of both
34 MAC3A and MAC3B in the *mac3b mac3b* double mutant reduces the accumulation of miRNAs, causing
35 elevated transcript levels of miRNA targets. *mac3a mac3b* also decreases the levels of primary miRNA
36 transcripts (pri-miRNAs). However, MAC3A and MAC3B do not affect the promoter activity of genes
37 encoding miRNAs (*MIR* genes), suggesting that they may not affect *MIR* transcription. This result
38 together with the fact that MAC3A associates with pri-miRNAs *in vivo* indicates that MAC3A and
39 MAC3B may stabilize pri-miRNAs. Furthermore, we find that MAC3A and MAC3B interact with the
40 DCL1 complex that catalyzes miRNA maturation, promote DCL1 activity and are required for the
41 localization of HYL1, a component of the DCL1 complex. Besides MAC3A and MAC3B, two other
42 MAC subunits, CDC5 and PRL1, also function in miRNA biogenesis. Based on these results, we propose
43 that MAC functions as a complex to control miRNA levels through modulating pri-miRNA transcription,
44 processing and stability.

45
46
47 **INTRODUCTION**

48 microRNAs (miRNAs), ~ 21-nucleotide in size, are endogenous non-coding RNAs that mainly
49 repress gene expression at post-transcriptional levels (Baulcombe, 2004; Axtell, 2013). They are

50 generated from the imperfect stem-loop residing in the primary miRNA transcripts (pri-miRNAs)
51 (Voinnet, 2009), most of which are produced by DNA-dependent RNA polymerase II (Xie et al.,
52 2005). In plants, the RNase III enzyme DICER-LIKE 1 (DCL1) slices pri-miRNAs at least two
53 times in the nucleus to release a miRNA-containing duplex (Baulcombe, 2004; Axtell, 2013;
54 Zhang et al., 2015). Then, the small RNA methyltransferase HUA ENHANCER1 (HEN1)
55 methylates the miRNA duplexes to protect them from degradation and untemplated uridine
56 addition (Zhai et al., 2013; Ren et al., 2014). Following methylation, the miRNA strand is
57 incorporated into the effector called ARGONAUTE 1 (AGO1) with the assistance from HEAT
58 SHOCK PROTEIN 90 and CYCLOPHILIN 40 and recognizes target transcripts through
59 sequence complementarity (Baumberger and Baulcombe, 2005; Vaucheret, 2008; Smith et al.,
60 2009; Earley and Poethig, 2011). AGO1 cleaves target mRNAs or inhibits their translation, and
61 therefore, represses gene expression.

62

63 Pri-miRNAs may be co-transcriptionally processed since DCL1 associates with *MIR* loci (Fang
64 et al., 2015a). In the past decades, protein factors that regulate miRNA biogenesis through
65 influencing pri-miRNA transcription, processing and stability have been identified in plants. The
66 transcriptional co-activator MEDIATOR (Kim et al., 2011), the CYCLIN-DEPENDENT
67 KINASES (CDKs) (Hajheidari et al., 2012), the transcription factor NEGATIVE ON TATA
68 LESS 2 (NOT2) (Wang et al., 2013), the DNA binding protein CELL DIVISION CYCLE 5
69 (CDC5) (Zhang et al., 2013) and ELONGATOR (Fang et al., 2015a) are required for optimized
70 Pol II activity at the *MIR* promoters. Following transcription, the forkhead domain-containing
71 protein DAWDLE (DDL) (Yu et al., 2008) and the WD-40 protein PLEIOTROPIC
72 REGULATORY LOCUS 1 (PRL1) (Zhang et al., 2014) bind pri-miRNAs to prevent their
73 degradation.

74

75 To efficiently and accurately process pri-miRNAs, DCL1 forms a complex with the double
76 stranded RNA (dsRNA)-binding protein HYPONASTIC LEAVES1 (HYL1), the Zinc-finger
77 protein SERRATE (SE) and the RNA-binding protein TOUGH (TGH) (Fang and Spector, 2007;
78 Fujioka et al., 2007; Song et al., 2007; Dong et al., 2008; Ren et al., 2012). The formation of the
79 DCL1 complex requires NOT2 (Wang et al., 2013), ELONGATOR (Fang et al., 2015a),
80 MODIFIER OF SNC1, 2 (MOS2, an RNA-binding protein) (Wu et al., 2013) and the DEAH-box

81 helicase PINP1 (Qiao et al., 2015). How MOS2 and PINP1 participate in the assembly of the
82 DCL1 complex remains unclear, since they do not interact with the DCL1 complex (Wu et al.,
83 2013; Qiao et al., 2015). Efficient loading of pri-miRNAs to the DCL1 complex requires TGH
84 (Ren et al., 2012), the THO/TREX complex that is involved in nuclear RNA transport
85 (Francisco-Mangilet et al., 2015), and the ribosome protein STV1 (Li et al., 2017). Notably,
86 several additional proteins including the CAP-BINDING PROTEINs (CBPs) (Gregory et al.,
87 2008; Laubinger et al., 2008), NOT2, ELONGATOR, DDL, CDC5 and PRL1 also associate with
88 the DCL1 complex to enhance pri-miRNA processing. In addition, SICKLE (SIC, a proline-rich
89 protein) (Zhan et al., 2012), RECEPTOR FOR ACTIVATED C KINASE 1 (RACK1) (Speth et
90 al., 2013), STABILIZED1 (STA1, a pre-mRNA processing factor 6 homolog) (Ben Chaabane et
91 al., 2013), REGULATOR OF CBF GENE EXPRESSION 3 (RCF3, also known as HOS5 and
92 SH11) (Chen et al., 2015; Karlsson et al., 2015) and GRP7 (a glycine-rich RNA-binding protein)
93 (Koster et al., 2014) also regulate miRNA biogenesis. However, they do not associate with
94 DCL1. Moreover, phosphorylation and dephosphorylation of HYL1 are crucial for pri-miRNA
95 processing (Manavella et al., 2012). In addition, protein factors that act in miRNA biogenesis are
96 also transcriptionally and post-transcriptionally regulated. For instance, DCL1 transcription is
97 modulated by the histone acetyltransferase GCN5 (Kim et al., 2009), STA1 (Ben Chaabane et al.,
98 2013) and the transcription factor XAP5 CIRCADIAN TIMEKEEPER (XCT) (Fang et al.,
99 2015b). Notably, HYL1 protein levels are maintained by the SNF1-RELATED PROTEIN
100 KINASE 2 (Yan et al., 2017) and the E3 ubiquitin ligase CONSTITUTIVE
101 PHOTOMORPHOGENIC 1 (COP1) (Cho et al., 2014) through unknown mechanisms. Recently,
102 KETCH1 (KARYOPHERIN ENABLING THE TRANSPORT OF THE CYTOPLASMIC
103 HYL1)-mediated transportation of HYL1 from the cytoplasm to the nucleus was shown to be
104 crucial for miRNA biogenesis (Zhang et al., 2017). Interestingly, pri-miRNA structures also
105 influence the DCL1 activity (Mateos et al., 2010; Song et al., 2010; Werner et al., 2010; Bologna
106 et al., 2013; Zhu et al., 2013). For instance, the internal loop below the miRNA/miRNA* within
107 the stem-loop is important for the processing of some pri-miRNAs.

108

109 Among proteins associated with the DCL1 complex, CDC5 and PRL1 are two core subunits of
110 the MOS4-associated complex (MAC) (Monaghan et al., 2009). MAC is a conserved complex
111 that associates with the spliceosome (Deng et al., 2016). Its homolog complexes in human and

112 yeast are known as the CDC5-SNEV^{Prp19-Pso4} (PRP19) complex and the Nineteen complex (NTC),
113 respectively (Palma et al., 2007). Both PRP19 and NTC function in splicing, DNA repair, cell
114 cycle and genome stability (Chanarat and Strasser, 2013). MAC contains three additional core
115 subunits, MAC3A, MAC3B and MOS4, and at least 13 accessory proteins with diversified
116 functions (Monaghan et al., 2009). Deficiency in MAC impairs plant immunity and development
117 (Monaghan et al., 2009). However, related mechanisms still need investigation. We have
118 previously shown that CDC5 and PRL1 have overlapping roles in regulating DCL1 activity, but
119 distinct functions in pri-miRNA transcription and stability (Zhang et al., 2013; Zhang et al.,
120 2014). These results raise the possibility that other MAC components may also have diversified
121 effects on miRNA biogenesis. Among core MAC components, MAC3A and MAC3B are two
122 homologous U-box type E3 ubiquitin ligases (~ 82% identity and 90% similarity) (Monaghan et
123 al., 2009). E3 ligase activity of MAC3B has been demonstrated *in vitro* (Wiborg et al., 2008).
124 We previously showed that a loss-of-function mutation in MAC3A does not affect miRNA
125 accumulation (Zhang et al., 2014). However, this result may reflect the redundant function of
126 MAC3B with MAC3A.

127

128 In this study, we found that lack of both MAC3A and MAC3B reduces the accumulation of
129 miRNAs and impairs the localization of HYL1 in the D-body. MAC3A associates with the
130 DCL1 complex and pri-miRNAs and promotes pri-miRNA processing. MAC3A and MAC3B
131 are also required for accumulation of pri-miRNAs. However, unlike CDC5, MAC3A neither
132 interacts with Pol II nor affects *MIR* transcription. These results suggest that MAC3A/3B may
133 stabilize pri-miRNAs and act as a co-factor to promote D-body formation and pri-miRNA
134 processing. In addition, we show that MAC3A is a phosphorylation-dependent E3 ligase and its
135 E3 ligase activity is required for miRNA biogenesis. We propose that MAC may act as a
136 complex to promote miRNA biogenesis and different MAC components may have distinct and
137 cooperative effects on pri-miRNA transcription, stability and processing.

138

139

140 **RESULTS**

141

142 **MAC3A and MAC3B are required for miRNA biogenesis**

143 The fact that CDC5 and PRL1, two core components of MAC are required for miRNA
144 biogenesis suggests that other MAC components may also function in miRNA biogenesis.
145 However, we previously showed that a single *mac3a* mutation does not affect miRNA
146 accumulation in *Arabidopsis thaliana* (Zhang et al., 2014). To evaluate if this result might reflect
147 redundancy between MAC3A and MAC3B in miRNA biogenesis, we generated a *mac3a mac3b*
148 double mutant through crossing *mac3a* (Salk_089300) to *mac3b* (Salk_050811) (Monaghan et
149 al., 2009). Compared with Col (wild-type plant, WT), *mac3a mac3b* displayed pleiotropic
150 development defects (Figure 1). For instance, the root length of *mac3a mac3b* is much shorter
151 (Figure 1A and I). Moreover, the size of the *mac3a mac3b* was smaller (Figure 1B). Reduced
152 cell number was likely responsible for the smaller size of *mac3a mac3b*, since the size of
153 palisade cells from *mac3a mac3b* was comparable to that from Col (Figure 1C, 1D and 1J). In
154 addition, *mac3a mac3b* leaves had three to four branch points (4–5 branches) on average, while
155 most trichomes of Col had two branch points (three branches)(Figure 1E, 1F and 1K).
156 Furthermore, the silique length of *mac3b mac3b* was shorter than that of Col (Figure 1G and 1L).
157 Moreover, the amounts of aborted seeds were higher in the siliques of *mac3a mac3b* than those
158 of WT (Figure 1H and 1M), suggesting that MAC3A and MAC3B also affect fertility.

159

160 The pleiotropic growth defects of *mac3a mac3b* are consistent with the effect of miRNAs on
161 plant development; we therefore examined the accumulation of miRNAs in *mac3a mac3b* and
162 Col through RNA gel blot. The abundance of all nine examined miRNAs was reduced in *mac3a*
163 *mac3b* relative to Col (Figure 2A). RT-quantitative PCR (RT-qPCR) analyses further confirmed
164 that miRNA levels were decreased in *mac3a mac3b* (Figure 2B). We also examined the effect of
165 MAC3A and MAC3B on trans-acting siRNAs (ta-siRNAs), which is another class of sRNAs that
166 represses gene expression at post-transcriptional levels (Peragine et al., 2004; Allen et al., 2005;
167 Yoshikawa et al., 2005; Axtell et al., 2006). Similar to miRNAs, ta-siR255 was reduced in
168 abundance in *mac3a mac3b* (Figure 2A). However, the effect MAC3A and 3B on ta-siR255
169 might be indirect, since the production of ta-siRNAs depending on miRNAs, whose abundance
170 was reduced in *mac3a mac3b*.

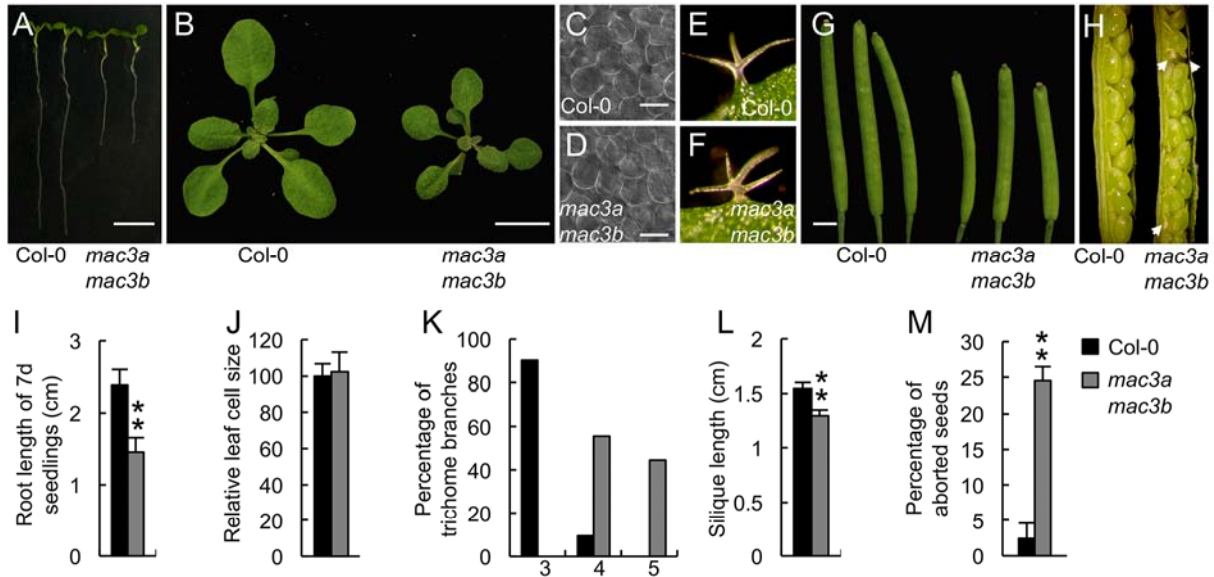


Figure 1. *mac3a mac3b* displays pleiotropic developmental defects.

(A) 7-day-old seedlings of Col and *mac3a mac3b*. Bar: 5 mm. (B) Three-week-old Col and *mac3a mac3b*. Bar: 1 cm. (C) and (D) Palisade cells of the fifth leaves from Col (C) and *mac3a mac3b* (D). Bar: 100 μ m. (E) and (F) Trichomes of Col and *mac3a mac3b*. Bar: 0.3 mm. (G) Mature siliques of Col and *mac3a mac3b*. Bar: 2mm. (H) Dissected siliques of Col and *mac3a mac3b*. White arrow: aborted seeds. (I) Quantification of root length in Col and *mac3a mac3b*. 30 plants were measured to calculate average root length. **: P<0.01 by Student's *t* test. (J) Quantification of cell size of the fifth leaves in Col and *mac3a mac3b*. The value of Col was set as 100. 80 cells of the fifth leaves from each genotype were measured. (K) Quantification of trichome branches in Col and *mac3a mac3b*. 60 trichomes from each genotype were analyzed. Numbers (3, 4, or 5) indicate the number of branches. (L) Quantification of silique length in Col and *mac3a mac3b*. 30 siliques from the same position of each genotype were measured. **: P<0.01 by Student's *t* test. (M) Quantification of aborted seeds in Col and *mac3a mac3b*. 20 siliques from Col or *mac3a mac3b* were analyzed. **: P<0.01 by Student's *t* test, compared to Col-0 value. Error bars in (I) to (M) indicate standard errors (SD).

171

172 We further compared miRNA profile from inflorescences of *mac3a mac3b* with that of WT
 173 through deep sequencing. The abundance of many miRNAs was reduced in *mac3a mac3b*
 174 relative to WT (Supplemental Figure 1A and Supplemental Data Set 1), suggesting that MAC3A
 175 MAC3B may have a global effect on miRNA accumulation. We also compared the effect of
 176 *mac3a mac3b* on miRNA accumulation with that of *dcl1-9* (a weak allele of *dcl* mutants) and
 177 *cdc5*. As expected, *cdc5* and *dcl1-9* reduced the abundance of most miRNAs (Supplemental
 178 Figure 1B, 1C and Supplemental Data Set 1). Among significantly down-regulated miRNAs
 179 (P<0.1), DCL1, CDC5 and MAC3A/MAC3B showed overlapping effects on many of them
 180 (Supplemental Figure 1D). However, some miRNAs were differentially affected by DCL1,
 181 CDC5 and MAC3A/MAC3B (Supplemental Figure 1D). These results suggest that these proteins
 182 may have overlapping and distinct roles in miRNA biogenesis.

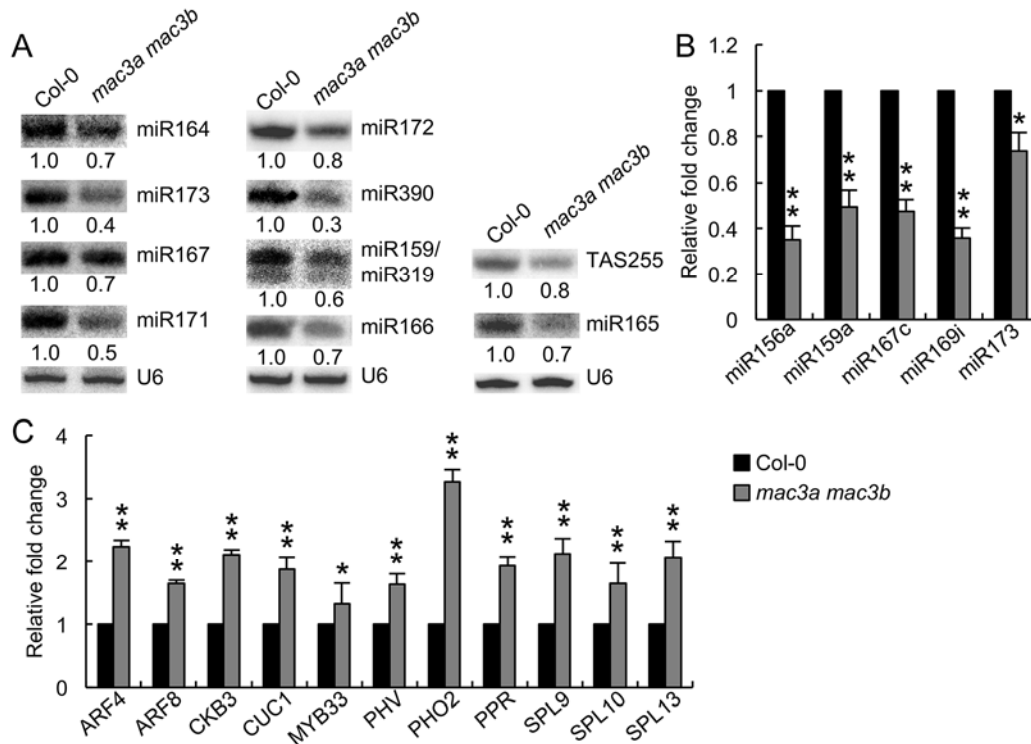


Figure 2. *mac3a mac3b* reduces the accumulation of miRNAs.

(A) The levels of small RNAs in Col and *mac3a mac3b* detected by RNA gel blot. *U6* RNA serves as the loading control. The numbers shown below the picture indicates the amount of small RNAs in *mac3a mac3b* relative to that of Col (set as 1) and represent mean of three replicates ($P < 0.05$). miR159/319: the upper band was miR159 and the lower band showed miR319. (B) The levels of miRNAs detected by RT-qPCR. miRNA levels in *mac3a mac3b* were normalized to those of *U6* RNA and compared with Col (value set as 1). Error bars: standard errors (SD) of three replicates (*: $P < 0.05$; **: $P < 0.01$ by Student's *t* test, compared to Col-0 value). (C) The transcript levels of miRNA targets in Col and *mac3a mac3b* detected by RT-qPCR. The transcript levels of miRNA targets were normalized to those of *UBIQUITIN 5 (UBQ5)* and compared with Col (set as 1). Error bars: standard errors (SD) of three replicates (**: $P < 0.01$ by Student's *t* test, compared to Col-0 value).

183

184 Next, we evaluated the influence of *mac3a mac3b* on the transcript levels of *ARF4*, *ARF8*, *CKB3*,
 185 *CUC1*, *MYB33*, *PHO2*, *PHV*, *PPR*, and *SPL9/10/13*, which are targets of tasiR-ARF, miR167,
 186 miR397, miR164, miR159, miR399, miR166, miR400, miR156, respectively. The levels of these
 187 target transcripts were increased in *mac3a mac3b* compared with Col (Figure 2C), suggesting
 188 that MAC3A and 3B are required for optimal activity of miRNAs and ta-siRNAs.

189

190 To determine if the lack of MAC3A and MAC3B was responsible for the observed phenotypes,
 191 we expressed a genomic copy of *MAC3A* fused with a *GUS* gene at its 3' end under the control of
 192 its native promoter (*proMAC3A:MAC3A-GUS*) in *mac3a mac3b*. The expression of this
 193 transgene rescued the developmental defects of *mac3a mac3b* (Supplemental Figure 2A). In

194 addition, fusion constructs *MAC3B-GFP* (*pro35S:MAC3B-GFP*) or *MYC-MAC3A*
195 (*pro35S:MYC-MAC3A*) under the control of the *35S* promoter also complemented the
196 developmental defects of *mac3a mac3b* (Supplemental Figures 2B and 2J). Consistent with this
197 observation, miRNA and target transcript levels in the complementation lines were comparable
198 to those in Col (Supplemental Figure 2K and 2L). We also examined the expression pattern of
199 MAC3A in *mac3a mac3b* harboring *proMAC3A:MAC3A-GUS* through GUS histochemical
200 staining. MAC3A was universally expressed and displayed high expression levels in primary
201 root tip, lateral root, and young leaves (Supplemental Figure 2C-2I). These results demonstrate
202 that MAC3A and MAC3B act redundantly to control development and miRNA accumulation of
203 Arabidopsis.

204

205 **MAC3A and MAC3B do not affect *MIR* transcription**

206 We have previously shown that CDC5 and PRL1 regulate pri-miRNA levels through modulating
207 pri-miRNA transcription and stability, respectively (Zhang et al., 2013; Zhang et al., 2014). This
208 led us to test if pri-miRNA levels were also altered in *mac3a mac3b*. As expected, all examined
209 pri-miRNAs were reduced in abundance in *mac3a mac3b* compared with Col (Figure 3A). We
210 suspected that as in *cdc5*, this reduction could be caused by alteration in transcription. Thus, we
211 evaluated the effect of *mac3a mac3b* on *MIR* promoter activity. The *MIR* promoter reporter
212 construct, *pMIR167a:GUS* (Zhang et al., 2014), was crossed into *mac3a mac3b*. Histochemical
213 staining and RT-qPCR analyses revealed that the expression levels of GUS in *mac3a mac3b*
214 were similar to those in WT (Figure 3B and 3C), indicating that MAC3A and MAC3B may have
215 no effect on *MIR* promoter activity. Furthermore, we tested the interaction between MAC3A and
216 the second largest subunit of Pol II (RPB2) through co-immunoprecipitation assay (Co-IP) in the
217 *mac3a mac3b* expression *pro35S:MAC3A-GFP*. In MAC3A-GFP precipitates, we did not detect
218 the presence of RPB2 (Figure 3D), suggesting that unlike CDC5 and PRL1, MAC3A does not
219 associate with RPB2. We also examined the occupancy of Pol II at the *MIR* promoters through
220 chromatin immunoprecipitation (ChIP) assays in *mac3a mac3b* and Col performed using anti-
221 RPB2 antibody. qPCR analysis did not detect an obvious difference of Pol II occupancy at
222 various *MIR* promoters between *mac3a mac3b* and Col (Figure 3E). Taken together, these results
223 suggest that MAC3A and MAC3B do not affect *MIR* transcription.

224

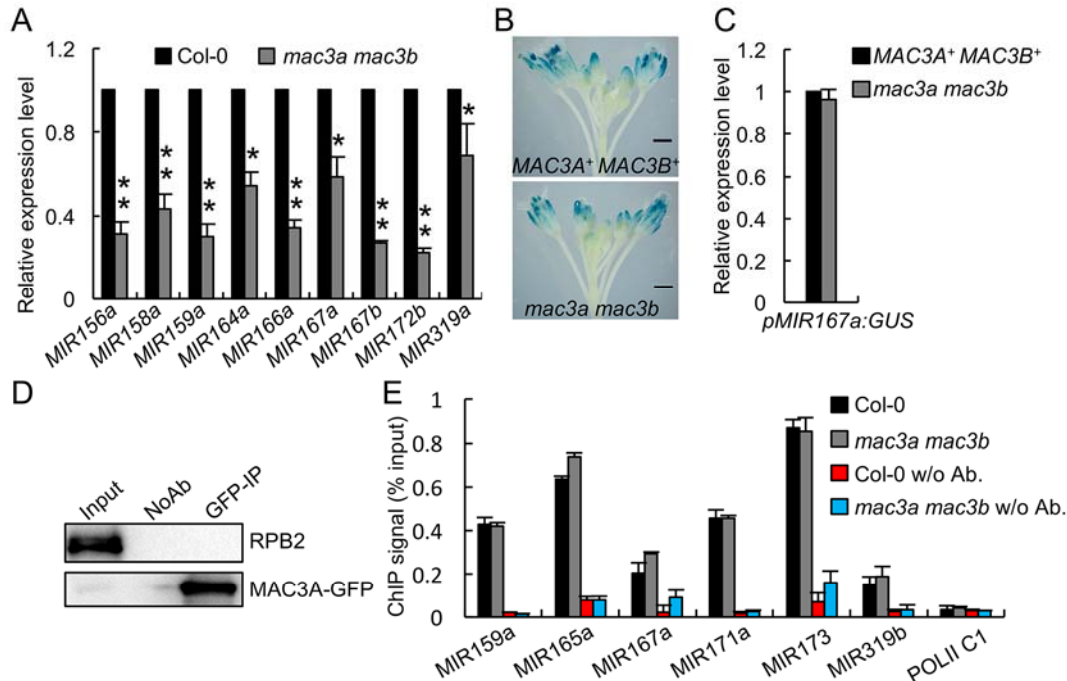


Figure 3. *mac3a mac3b* reduces the accumulation of pri-miRNAs without affecting transcription.

(A) The levels of pri-miRNAs in Col and *mac3a mac3b*. RT-qPCR was used to analyze pri-miRNA levels. Pri-miRNA levels in *mac3a mac3b* were normalized to those of *UBQ5* and compared with Col (Values were set as 1). Error bars indicate standard errors (SD) of three replicates (*: $P < 0.05$; **: $P < 0.01$ by Student's *t* test, compared to Col-0 value). (B) Histochemical staining of GUS in Col and *mac3a mac3b* harboring *proMIR167a:GUS*. 15 plants containing *GUS* were analyzed for each genotype. A representative image for each genotype is shown. Bar: 2 mm. (C) *GUS* transcript levels in Col and *mac3a mac3b* harboring the *proMIR167a:GUS* transgene. *GUS* transcript levels detected by RT-qPCR were normalized to those of *UBQ5* and compared with Col (Value was set as 1). Error bar: standard errors (SD) of three replicates. (D) MAC3A does not co-immunoprecipitate with RPB2. Anti-GFP antibody was used to immunoprecipitate MAC3A-GFP. MAC3A-GFP and RPB2 were detected with anti-GFP and anti-RPB2 antibodies, respectively. Input: Total proteins before IP. NoAb: Immunoprecipitates with agarose beads. (E) The occupancy of Pol II at *MIR* promoters in Col and *mac3a mac3b* detected by ChIP followed by qPCR. The intergenic region between At2g17470 and At2g17460 (POL II C1) was used as a negative control.

225 MAC3A and MAC3B associate with the DCL1 complex

226 To further understand how MAC3A and MAC3B affect miRNA biogenesis, we examined the
 227 effect of *mac3a mac3b* on the expression of *DCL1*, *DDL*, *SE*, *HYL1*, *CBP20/80* and *HEN1*,
 228 which are known to function in miRNA biogenesis. The transcript levels of *HYL1*, and
 229 *CBP20/80* were slightly increased, while the abundance of *DDL* transcripts was marginally
 230 reduced (Supplemental Figure 3A). In addition, the levels of *DCL1*, *HEN1* and *SE* did not show
 231 significant change. Immunoblot analyses further showed that the protein levels of *SE* and *DCL1*
 232 were not changed in *mac3a mac3b* whereas the *HYL1* protein was slightly increased in
 233 abundance (Supplemental Figure 3B). Moreover, we also examined the effect of *mac3a mac3b*
 234 on the splicing of *DCL1*, *DDL*, *HEN1*, *HYL1* and *SE* using RT-PCR with primers targeting a

235 subset of introns (Supplemental Figure 3C). MAC3A and MAC3B did not have an obvious
236 effect on the splicing of these introns (Supplemental Figures 3C and 3D). However, it is not clear
237 if MAC3A and MAC3B affect the splicing of other introns in these examined genes.

238
239 Since MAC3A and MAC3B are components of the MAC, we suspected that like CDC5 and
240 PRL1, MAC3A and MAC3B might also interact with the DCL1 complex. We performed a
241 bimolecular fluorescence complementation (BiFC) assay to test this possibility. In the leaves of
242 *N. benthamiana* transiently co-expressing MAC3A or MAC3B fused with the C-terminal
243 fragment of cyan fluorescent protein (cCFP) with CDC5, PRL1, DCL1 or SE fused with the N-
244 terminal fragment of Venus (nVenus), yellow fluorescence signals were observed (shown in
245 green color; Figure 4A and Supplemental Figure 4). BiFC signals of MAC3A or MAC3B with
246 PRL1, DCL1 and SE were localized at the discrete bodies (Figure 4A and Supplemental Figure
247 4). Interestingly, the interaction between MAC3A/3B and CDC5 produced not only discrete
248 signals but also diffused ones, agreeing with the role of MAC in mRNA splicing (Figure 4A and
249 Supplemental Figure 4). Co-expression cCFP-MAC3A or cCFP-3B with nVenus-HYL1 resulted
250 in weak and diffused YFP signals (Figure 4A and Supplemental Figure 4), consistent with the
251 observation that CDC5 and PRL1 do not co-immunoprecipitate with HYL1 (Zhang et al., 2014).

252
253 Next, we used co-IP to confirm the interaction of MAC3A with CDC5, PRL1, DCL1 and SE.
254 We first co-expressed MYC-MAC3A with CDC5-YFP, PRL1-YFP or YFP and performed IP
255 with anti-YFP antibodies. MYC3A was detected in CDC5-YFP and PRL1-YFP precipitates, but
256 not in YFP precipitates (Figure 4B and 4C), confirming the interaction of MAC3A with CDC5
257 and PRL1. We next co-expressed MAC3A-GFP or GFP with MYC-DCL1 or MYC-SE and
258 tested the interaction of co-expressed proteins. MAC3A-YFP, but not YFP, co-IPed with MYC-
259 DCL1 and MYC-SE (Figure 4D and 4E). Furthermore, RNase A treatment did not disrupt the
260 interaction of MAC3A with DCL1 and SE (Figure 4B-4D). These results suggest that MAC3A
261 and MAC3B associate with the DCL1 complex in an RNA-independent manner.

262 263 ***mac3a mac3b* reduces pri-miRNA processing *in vitro***

264 The association of MAC3A and MAC3B suggests that they may modulate DCL1 activity.

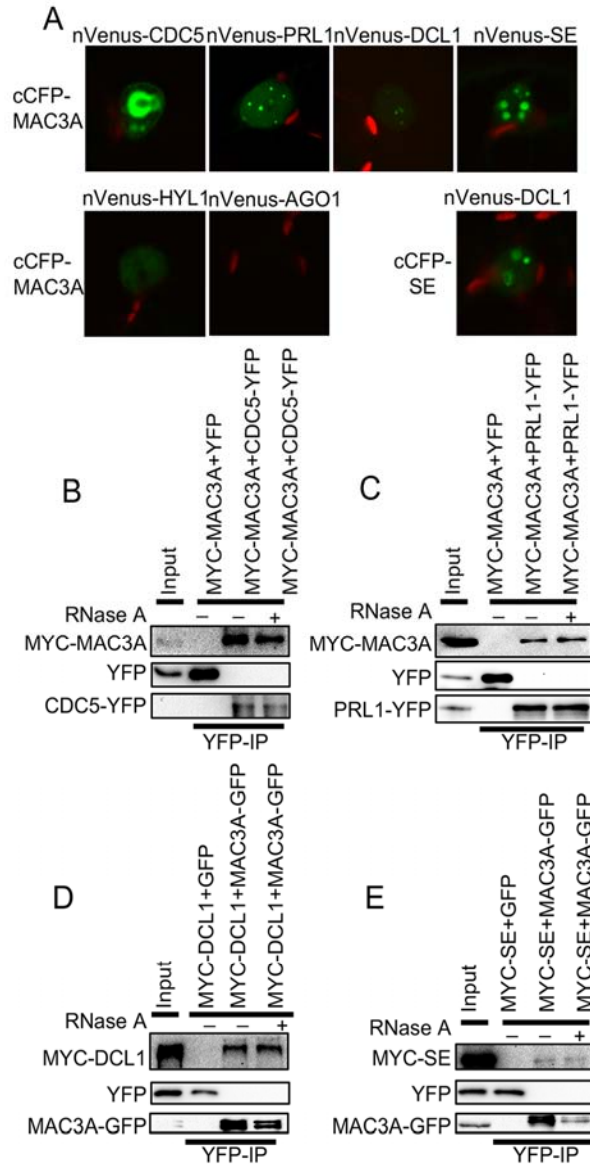


Figure 4. MAC3A associates with the DCL1 complex.

(A) The interaction of MAC3A with CDC5, PRL1, DCL1, HYL1, SE and AGO1 detected by BiFC analysis. Paired cCFP- and nVenus-fusion proteins were co-expressed into *N. benthamiana* leaves. Green color indicates the BiFC signal (originally yellow fluorescence) detected by a confocal microscopy at 48 hour after infiltration. 100 nuclei were examined for each pair and a representative image is shown. Red: autofluorescence of chlorophyll. (B) Co-immunoprecipitation (Co-IP) between MAC3A and CDC5. (C) Co-IP between MAC3A and PRL1. CDC5-YFP, PRL1-YFP or YFP were co-expressed with MYC-MAC3A in *N. benthamiana*. IP was performed using anti-YFP antibodies. MYC-MYC3A, CDC5-YFP, PRL1-YFP and YFP were detected by immunoblot. (D) Co-IP between MAC3A and DCL1. (E) Co-IP between MAC3A and SE. GFP or MAC3A-GFP was co-expressed in *N. benthamiana* with MYC-DCL1 or MYC-SE, respectively. IP was performed using an anti-MYC antibody. After IP, proteins were detected by immunoblot. Inputs in (B) to (E) show the total protein before IP. RNase A was used to digest RNA stands.

265 We used an *in vitro* pri-miRNA processing assay to test this possibility. As previously described,
 266 we first generated a radiolabeled pri-miR162b (*MIR162b*) composed of the stem-loop of

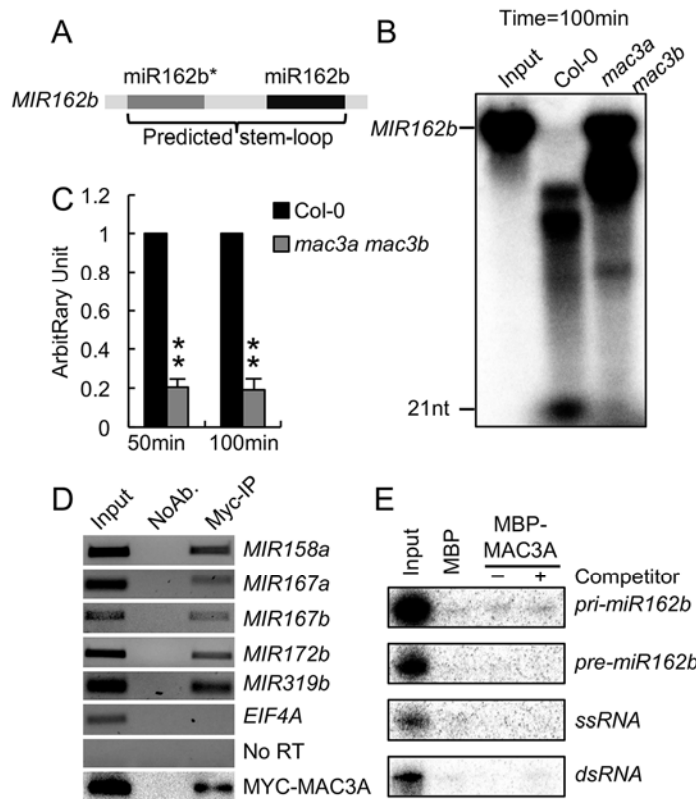


Figure 5. MAC3A associates with pri-miRNAs and promotes pri-miRNA processing.

(A) Diagram of *MIR162b* used in the *in vitro* processing assay. (B) *MIR162b* processing in protein extracts from *mac3a mac3b* and Col. (C) Quantification of miR162 production in *mac3a mac3b* extracts relative to Col. The processing reaction was performed for 50 or 100 min. The radioactive signal of miR162 was normalized to input in *mac3a mac3b* and compared with that in Col (value set as 1). The value is the mean of three repeats. **: $P < 0.01$ by Student's *t* test, compared to Col-0 value. (D) MAC3A interacts with pri-miRNAs *in vivo*. RIP assay was performed on transgenic plants harboring *pro35S:MYC-MYC3A* using an anti-MYC antibody. 5 percent RNAs were used as the input. NoAb: No antibody control. (E) MAC3A does not bind RNAs *in vitro*. *Pri-miR162b*, *pre-miR162b*, ssRNA and dsRNA were generated through *in vitro* transcription. ssRNA represents single-stranded RNA; dsRNA indicates double-stranded RNA.

267 miR162b with 6-nt arms at each end using *in vitro* transcription (Figure 5A). Processing of
 268 *MIR162b* was then tested in the protein extracts from young flowers of *mac3a mac3b* or Col.
 269 The production of miR162b from *MIR162b* was reduced in the protein extracts of *mac3a mac3b*
 270 relative to Col (Figure 5B). At 50 min and 100 min time points, the levels of miR162 generated
 271 in *mac3a mac3b* were ~ 20% of those produced in Col (Figure 5C). These results suggest that
 272 MAC3A/3B may be required for the optimal activity of the DCL1 complex.

273

274 **MAC3A binds pri-miRNAs *in vivo***

275 The WD domain of MAC3A and MAC3B is known to mediate protein–protein interaction.

276 However, it can also interact with RNAs (Lau et al., 2009). Thus, it is possible that MAC3A and

277 MAC3B could bind pri-miRNAs. To test this hypothesis, we performed an RNA
278 immunoprecipitation assay (RIP) on seedlings of the *mac3a mac3b* complementation line
279 harboring the MYC-MAC3A transgene (Ren et al., 2012). Following cross-linking, nuclear
280 isolation, and immunoprecipitation, we examined the presence of pri-miRNAs in MAC3A IPs
281 using RT-PCR. All examined pri-miRNAs, but not the control *EIF4A* RNAs, were enriched in
282 the MAC3A IPs (Figure 5D). By contrast, pri-miRNAs were not detected in the no-antibody
283 controls (Figure 5D). These results suggest that MAC3A/3B associates with pri-miRNAs *in vivo*.

284
285 Next, we tested if MAC3A could directly bind pri-miRNA *in vitro* using the RNA pull-down
286 assay (Ren et al., 2012). In this assay, MBP and recombinant MAC3A fused with maltose-
287 binding protein (MBP) at its N-terminus (MBP-MAC3A) were expressed in *E. coli*, purified with
288 amylose resin, and then incubated with [³²P]-labeled *MIR162b* (Supplemental Figure 5A and
289 Figure 5E). After washing, neither MBP-MAC3A nor MBP retained *MIR162b* (Figure 5E).
290 MBP-MAC3A also did not interact with a ~100-nt single-stranded RNA (ssRNA), which was
291 generated through *in vitro* transcription using a N-terminal fragment of the *UBIQUITIN 5* (*N-*
292 *UBQ5*), or a dsRNA generated through annealing of sense and anti-sense strands of *N-UBQ5*
293 (Figure 5E). Because MAC3A activity needs phosphorylation (see below), we treated the
294 recombinant MAC3A protein with extracts from Col (see below) to modify the protein and then
295 tested its interaction with *MIR162b*. The modified MAC3A also did not interact with RNAs
296 (Supplemental Figure 5B). These results suggest that MAC3A is not an RNA-binding protein.

297

298 **MAC3A and MAC3B are required for the localization of HYL1 in D-bodies**

299 The interaction of MAC3A/B with the DCL1 complex also prompted us to test the effect of
300 *mac3a mac3b* on the formation of the D-body. We crossed a HYL1-YFP transgenic line, which
301 has been used as a reporter for the D-body (Wang et al., 2013; Wu et al., 2013; Qiao et al., 2015),
302 into *mac3a mac3b* and examined the percentage of cells containing D-bodies in the root tips and
303 elongation region. As previously reported (Wu et al., 2013), the HYL1-containing D-bodies
304 existed in most cells (~ 84%, Figure 6A, 6B and Supplemental Figure 6A and 6B) in WT. By
305 contrast, D-bodies were observed in only ~ 26% of cells in *mac3a mac3b*. This result
306 demonstrates that MAC3A and MAC3B are required for correct HYL1 localization, indicating
307 their potential role in facilitating D-body formation.

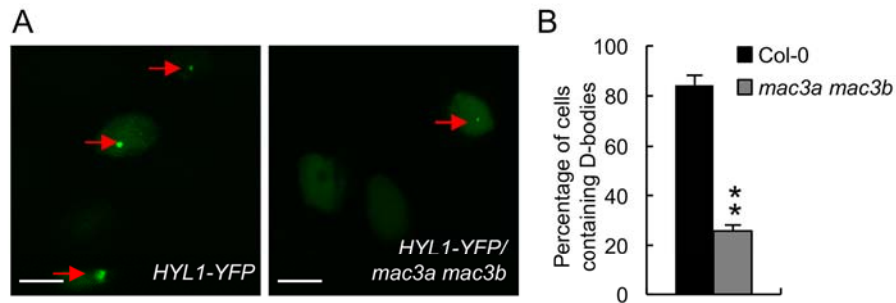


Figure 6. *mac3a mac3b* affects the localization of HYL1 in the nucleus.

(A) Image of HYL1 localization in the root cells of Col and *mac3a mac3b*. 7-day-old plants were examined. A typical image is shown. Arrows indicate the D-bodies. Bar: 5 μ m. (B) Quantification of root cells harboring HYL1-localized D-bodies in Col and *mac3a mac3b*. More than 400 cells from 12 roots for each genotype were examined. Error bar: standard deviation (n=400). **: P<0.01 by Student's *t* test, compared to Col-0 value.

308

309 **MAC3A is a U-Box ubiquitin E3 ligase whose activity depends on phosphorylation**

310 Both MAC3A and MAC3B contain an N-terminal ligase U-box domain that confers E3 ubiquitin
 311 ligase activity and recruits the E2 conjugating enzyme, a coiled-coil region that exists in all
 312 Prp19 homologs, mediates the tetramerization of Prp19 and interacts with CDC5L and SFP27 in
 313 metazoans, and a C-terminal WD domain composed of seven WD repeats that is required for
 314 substrate recruitment (Figure 7A). Homologous of MAC3A and MAC3B exist in all plants,
 315 while their copy numbers vary among different genomes (Supplemental Figure 7 and
 316 Supplemental Data Set 2).

317

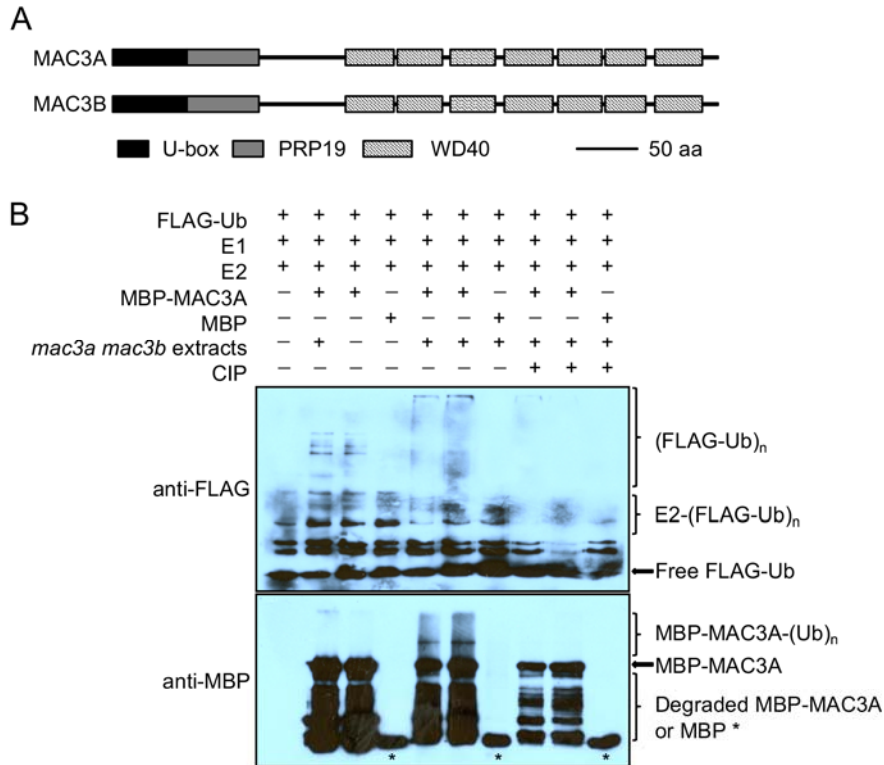


Figure 7. MAC3A is a *bona fide* U-box ubiquitin E3 ligase.

(A) The protein domains of MAC3A and MAC3B. (B) Ubiquitin ligase activity of MAC3A. The *in vitro* ubiquitin ligase activity assay was performed under the presence of FLAG-ubiquitin (FLAG-Ub), recombinant E1 and E2. MBP and no E3 ligase protein serve as negative controls. Poly-ubiquitination of MAC3A demonstrates its ubiquitin ligase activity. Anti-FLAG antibody and anti-MBP antibody were used to detect FLAG-ubiquitin and MBP/MBP-MAC3A, respectively.

318 Because MAC3A has considerable sequence difference from MAC3B, we tested if it is a
 319 ubiquitin E3 ligase using MBP-MAC3A (Supplemental Figure 5A). We examined the E3 ligase
 320 activity in the presence of ubiquitin, the ubiquitin-activating enzyme (E1) SIUBA and the
 321 ubiquitin-conjugating enzyme (E2) UBC8 (Zhou et al., 2017). However, MBP-MAC3A
 322 displayed only weak activity (Figure 7B). We suspected that like some other E3 ligases, MAC3A
 323 activity might depend on post-translational modification (Wang et al., 2015). Thus, we treated
 324 MBP-MAC3A and MBP protein with total protein extracts from inflorescences of *mac3a mac3b*.
 325 The use of *mac3a mac3b* was to avoid contamination from endogenous MAC3A/3B, since
 326 MAC3A potentially interacts with MAC3B. The treatment greatly improved MAC3A activity
 327 (Figure 7B). Notably, Alkaline Phosphatase (Calf intestinal phosphatase, CIP) treatment of
 328 MAC3A after incubation with *mac3a mac3b* protein extracts completely eliminated MAC3A
 329 activity (Figure 7B). These results demonstrate that MAC3A is a *bona fide* ubiquitin E3 ligase
 330 and that its activity depends on protein phosphorylation.

331
332
333
334
335
336
337
338
339
340
341
342
343
344
345
346
347
348
349
350

The ubiquitin ligase activity of MAC3A is required for miRNA and pri-miRNA accumulation

Since MAC3A is a ubiquitin ligase, we next asked if its function in miRNA biogenesis requires this activity. Based on the fact that the U-box domain of Prp19-like family is conserved in eukaryotes (Ohi et al., 2003), we generated two mutant versions of MAC3A in U-box domain through site-directed mutagenesis. In one mutant, the conserved amino acids of Tyrosine (Y) at position 23 and Glutamic acid (E) at position 24 were replaced with Glycine (G) and Alanine (A) (MAC3A^{Mut1}), respectively, while in the other one, the conserved amino acids of Histidine (H) at position 31 and Aspartic acid (D) at position 34 were replaced with Alanines (AA) (MAC3A^{Mut2}) (Figure 8A). These two mutations disrupted the ubiquitin ligase activity of MAC3A (Supplemental Figure 8A). To evaluate the effect of MAC3A^{Mut1} and MAC3A^{Mut2} on miRNA biogenesis, we generated stable transgenic lines in *mac3a mac3b* expressing MAC3A^{Mut1} or MAC3A^{Mut2} under the control of 35S promoter. The expression MAC3A^{Mut1} or MAC3A^{Mut2} did not rescue the developmental defects of *mac3a mac3b* (Supplemental Figure 8B and Figure 8B). Agreeing with this observation, the accumulation of both pri-miRNAs and miRNAs in *mac3a mac3b* was not recovered by MAC3A^{Mut1} or MAC3A^{Mut2} (Figure 8C and 8D). These results suggest that the ubiquitin ligase activity of MAC3A is required for miRNA biogenesis.

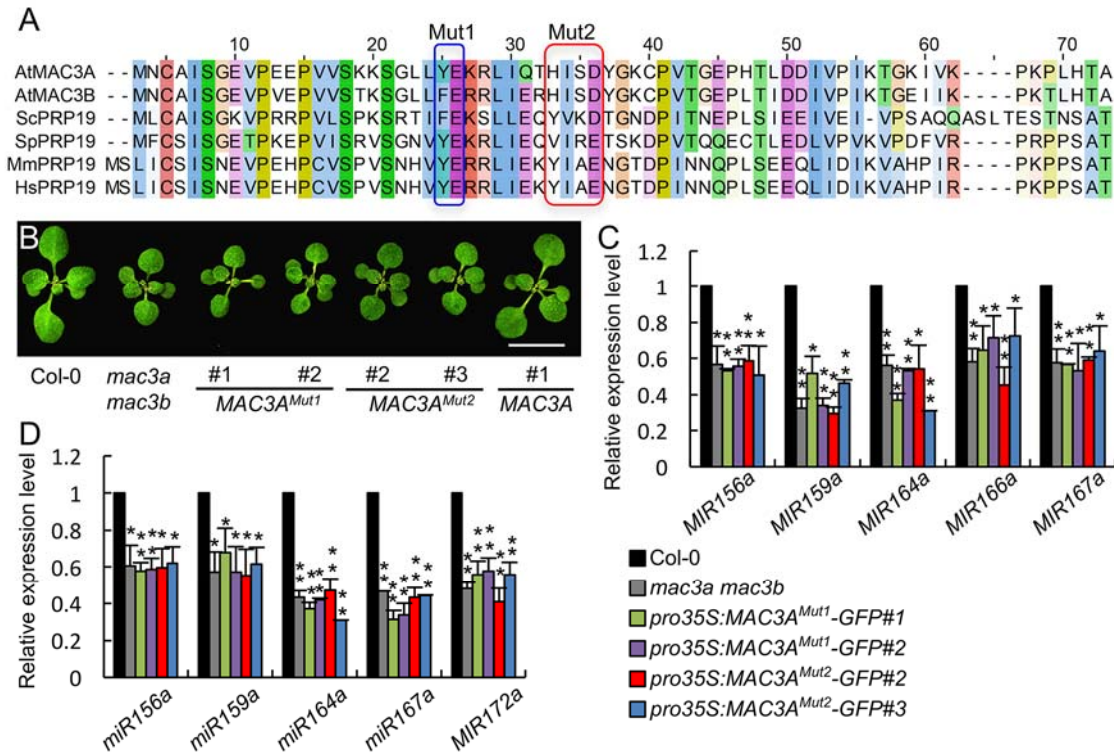


Figure 8. E3 ubiquitin ligase activity is required for MAC3A function in miRNA biogenesis.

(A) The aligned sequences of conserved U-box domain in MAC3A orthologs. The two mutated sites are shown in blue and red boxes, respectively. (B) 14-day-old seedlings of Col, *mac3a mac3b* and transgenic *mac3a mac3b* harboring *pro35S:MAC3A^{Mut1}-GFP* or *pro35S:MAC3A^{Mut2}-GFP* constructs. Two individual transgenic lines of each construct are shown. The transgenic line harboring *pro35S:MAC3A-GFP* is shown as control. Bar: 1 cm. (C) and (D) The pri-miRNA (C) and miRNA (D) levels in Col, *mac3a mac3b*, *35S:MAC3A^{Mut1}-GFP* transgenic plants, and *pro35S:MAC3A^{Mut2}-GFP* transgenic plants detected by RT-qPCR. Pri-miRNA levels in *mac3a mac3b* and transgenic plants were normalized to those of *UBQ5* and compared with Col (values were set as 1). miRNA levels in *mac3a mac3b* and transgenic plants were normalized to those of *U6* RNA and compared with Col (value set as 1). Error bars: standard errors (SD) of three replicates (*: $P < 0.05$; **: $P < 0.01$ by Student's *t* test, compared to Col-0 value).

351 DISCUSSION

352 MAC3A and MAC3B are conserved U-box type ubiquitin E3 ligases. In plants, MAC3A and
 353 MAC3B play important roles in plant immunity and development, and their counterparts in other
 354 organisms are required for splicing. In Arabidopsis, the MAC also associates with the
 355 spliceosome. However, only a few genes display moderated splicing in defects in *mac3a mac3b*
 356 (Monaghan et al., 2010; Xu et al., 2012). Consequently, how MAC3A and MAC3B regulate
 357 development and immunity remains elusive. In this study, we show that the accumulation of
 358 miRNA is reduced in *mac3a mac3b*. Furthermore, MAC3A and MAC3B associate with the
 359 DCL1 complex and pri-miRNAs. These results suggest that MAC3A and MAC3B are important
 360 players in miRNA biogenesis, in addition to their role in splicing. Impaired miRNA biogenesis

361 may partially explain the pleiotropic developmental defects of *mac3a mac3b*, since miRNAs
362 target many genes that are required for proper development.

363
364 There are at least three possible explanations for the decreased pri-miRNA levels in *mac3a*
365 *mac3b*. First, *mac3a mac3b* may have reduced *MIR* transcription. The facts that *mac3a mac3b*
366 does not show altered *MIR* promoter activity and that MAC3A does not co-IP with Pol II suggest
367 that MAC3A and MAC3B may not affect *MIR* transcription. However, we cannot rule out the
368 possibility that MAC3A and MAC3B influence *MIR* elongation or termination. Second,
369 enhanced pri-miRNA processing in *mac3a mac3b* may also decrease pri-miRNA accumulation.
370 However, reduced pri-miRNA processing is observed in *mac3a mac3b*, arguing against this
371 possibility. Third, *mac3a mac3b* may have reduced stability of pri-miRNAs (Figure 9). We give
372 this option more weight, given the observations that MAC3A associates with pri-miRNAs *in vivo*
373 and interacts with PRL1, which protects pri-miRNAs from degradation. It is reasonable to
374 speculate that MAC3A may stabilize pri-miRNAs through modulating the function of PRL1.
375 Indeed, it has been observed that the interaction between PRP19 (a MAC3A ortholog) and the
376 RNA-binding protein CWC2 is required for the stabilization of small nuclear RNAs (snRNAs)
377 related to splicing in yeast (McGrail et al., 2009; Vander Kooi et al., 2010).

378

379 MAC3A/MAC3B interacts with DCL1 and SE but appears to have weak or no association with
380 HYL1. Interestingly, a lack of MAC3A and MAC3B impairs the localization of HYL1 at the D-
381 body. How does this happen? One possibility is the decreased pri-miRNAs in *mac3a mac3b* may
382 affect the formation of D-body. However, loss-of-function mutants *mos2* and *pinp1*, in which the
383 levels of pri-miRNAs are increased or unaltered, respectively, also display impaired HYL1
384 localization or D-body assembly, arguing against this possibility. In human, PRP19-mediated
385 ubiquitination regulates the protein–protein interaction of the spliceosome, which is important
386 for the spliceosome assembly (Das et al., 2017). In addition, PRP19 also promotes the
387 recruitment of ATRIP (a kinase) to the DNA damage site through modifying DNA replication
388 protein A (Marechal et al., 2014). Thus, it is possible that MAC3A and MAC3B may influence
389 the recruitment of HYL1 through modifying proteins involved in D-body assembly.
390 Alternatively, they may co-transcriptionally facilitate the recruitment of the D-body to the

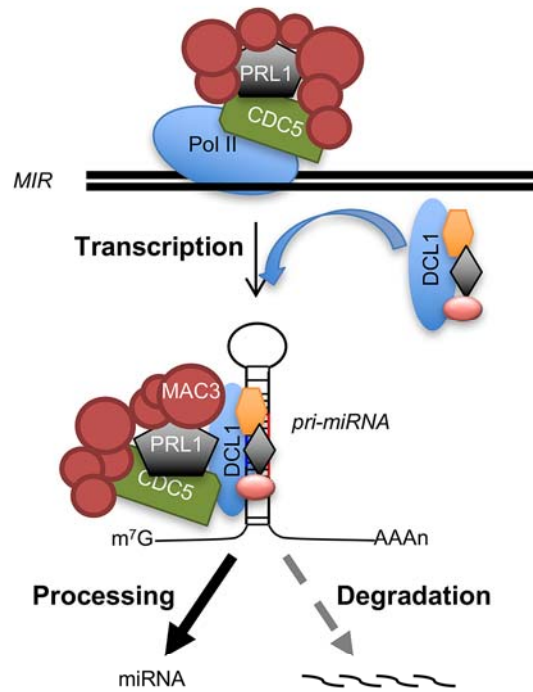


Figure 9. Proposed model for MAC function in miRNA biogenesis.

MAC is required for pri-miRNA transcription, processing, and stability. Some MAC components such as CDC5 interact with the *MIR* promoter and Pol II to positively regulate *MIR* transcription. Following transcription, MAC binds pri-miRNAs to prevent their turnover and functions as a co-factor to promote pri-miRNA processing. The MAC may also facilitate the recruitment of the DCL1 complex to the processing sites. Because the MAC contains subunits with diversified functions, individual MAC components may contribute distinctly and synergistically to miRNA biogenesis. Lack of the MAC results in reduced pri-miRNA transcription, stability, and/or processing.

391 processing site of pri-miRNAs (Figure 9). The association of MAC3A/3B with the DCL1
 392 complex is consistent with these hypotheses.

393

394 Pri-miRNA processing is also reduced in *mac3a mac3b*. This cannot be attributed to altered
 395 expression of genes involved in miRNA biogenesis, as the levels of these genes are either
 396 slightly increased or unaltered in *mac3a mac3b*. We have shown the CDC5 promotes DCL1
 397 activity through its interaction with the regulatory domains of DCL1 (Zhang et al., 2013), while
 398 PRL1 functions an accessory factor to facilitate CDC5 function in modulating DCL1 activity
 399 (Zhang et al., 2014). By analogy, MAC3A and MAC3B may function as components of the
 400 MAC to directly or indirectly enhance the DCL1 activity (Figure 9). Alternatively, impaired
 401 HYL1 localization or D-body formation may affect the DCL1 activity.

402

403 In summary, we find that MAC3A and MAC3B, two core components of the MAC, act
404 redundantly in miRNA biogenesis. They associate with the DCL1 complex, positively modulate
405 pri-miRNA accumulation, facilitate HYL1 localization at the D-body and enhance DCL1
406 activity. More importantly, we show that MAC3A is a phosphorylation-dependent ubiquitin
407 ligase and that this ligase activity is required for miRNA biogenesis. This result indicates that
408 certain signals may modulate MAC3A activity through phosphorylation and thereby regulate
409 miRNA accumulation. The involvement of four MAC core components in miRNA biogenesis
410 suggests that the MAC functions as a complex to promote miRNA biogenesis.

411 Besides core components, the MAC also contains at least 13 accessory components. The core
412 and accessory components of the MAC are proteins with diversified functions, such as
413 transcription factors, RNA-binding proteins, ubiquitin ligase, helicases, chromatin protein, WD
414 proteins, protein–protein interaction regulators, coiled-coil domain-containing proteins and zinc-
415 finger-domain-containing proteins. Moreover, the accessory components are dynamically
416 associated with the core complex, and sub-complexes with different functions are often formed.
417 Thus, it is likely that various MAC components act individually and coordinately in miRNA
418 biogenesis through influencing pri-miRNA transcription, processing, and stability and/or likely
419 have a role in the assembly of D-body (Figure 9), which resembles the diversified function of
420 PRP19 in splicing. Consistent with this notion, CDC5 and PRL1 contribute differently to pri-
421 miRNA accumulation but act as a complex to regulate DCL1 activity. It will be interesting to
422 further determine the functional mechanism of these proteins as individual components and as a
423 complex in miRNA biogenesis. The functions of the PRP19 complex from metazoans in
424 splicing, transcription, chromatin stability and lipid droplet biogenesis have been well
425 documented (Chanarat and Strasser, 2013). However, its function in metazoan miRNA
426 biogenesis is unknown. Given the fact that all four MAC components associate with SE, an
427 ortholog of ARS2, which is a key component of miRNA biogenesis in metazoa, it will not be
428 surprising if the PRP19 complex plays a role in metazoan miRNA biogenesis.

429
430

431 **METHODS**

432 **Plant materials and growth conditions**

433 SALK_089300 (*mac3a*) (Monaghan et al., 2009) and SALK_050811 (*mac3b*) were obtained
434 from the Arabidopsis Biological Resources Center (ABRC). They are in the Columbia (Col)
435 genetic background. Transgenic lines containing a single copy of *proMIR167a:GUS* or
436 *pro35S:HYL1-YFP* were crossed to *mac3a mac3b*. In the F2 generation, WT plants or *mac3a*
437 *mac3b* harboring *proMIR167a:GUS* or *pro35S:HYL1-YFP* were selected through PCR-based
438 genotyping for *mac3a*, *mac3b*, *GUS* or *GFP*. ~ 15 WT or *mac3a mac3b* plants were pooled for
439 GUS transcript level analyses. All plants were grown at 22°C with 16 hour light (cool white
440 fluorescent lamps, 25-W Sylvania 21942 FO25/741/ECO T8 linear tube) and 8 hour dark cycles.

441

442 **Plasmid construction**

443 A DNA fragment containing 2066 bp promoter and 3841bp coding region of *MAC3A* was PCR
444 amplified using DNAs from Col as templates with the primers of proMAC3A-4F and
445 MAC3AcDs-1R. The resulting PCR product was cloned into pENTR/D-TOPO vector and
446 subsequently cloned into pMDC163 binary vector to generate the *proMAC3A:MAC3A-GUS*
447 plasmid. The *MAC3A* full-length cDNA was RT-PCR amplified with the primers of
448 MAC3AcDs-1F and MAC3AcDs-1R, cloned into pENTR/D-TOPO vector and subcloned into
449 pEarleyGate203 or pMDC83 to generate the *pro35S:MYC-MAC3A* construct or the
450 *pro35S:MAC3A-GFP* construct. The *MAC3B* full-length cDNA was amplified with the primers
451 of MAC3BcDs-1F and MAC3BcDs-1R by RT-PCR and cloned into pENTR/D-TOPO vector and
452 subcloned into pMDC83 to generate the *pro35S:MAC3B-GFP* construct. To construct *cCFP-*
453 *MAC3A* or *cCFP-MAC3B*, *MAC3A* cDNA or *MAC3B* cDNA was PCR amplified using the
454 primer pair MAC3A-3F/2R or MAC3B-3F/2R, respectively, and cloned into pSAT4-cCFP-C
455 vector. Then, the *pro35S:cCFP-MAC3A* fragment or the *pro35S:cCFP-MAC3B* fragment was
456 released by I-SceI restriction enzyme digestion and subcloned to pPZP-RCS2-ocs-bar-RI vector.
457 The constructs cCFP-SE, nVenus-DCL1, nVenus-HYL1, nVenus-SE, and nVenus-AGO1 were
458 described previously (Ren et al., 2012). To construct *MBP-MAC3A*, the *MAC3A* cDNA sequence
459 was amplified with primer MAC3A-5F(Not1) and MAC3A-5R(Sal1) and subsequently inserted
460 into the pMAL-C5X vector. Site-mutagenesis of *MAC3A* was performed according the protocol
461 of QuikChange II Site-Directed Mutagenesis Kit (Agilent). The primers are list in Supplemental

462 Table 1.

463

464 **Plant complementation**

465 The *proMAC3A:MAC3A-GUS*, *pro35S:MYC-MAC3A*, *pro35S:MAC3A^{Mut1}-GFP*,
466 *pro35S:MAC3A^{Mut2}-GFP*, and *pro35S:MAC3B-GFP* plasmids were transformed into *mac3a*
467 *mac3b* using Agrobacterium-mediated floral dip method, respectively. The transgenic plants
468 harboring *proMAC3A:MAC3A-GUS*, *pro35S:MAC3A^{Mut1}-GFP*, *pro35S:MAC3A^{Mut2}-GFP*, or
469 *pro35S:MAC3B-GFP* were selected on MS medium containing hygromycin (30 µg/mL).
470 *pro35S:MYC-MAC3A* transformants were selected by spraying seedlings with 120 mg/L BASTA
471 solution.

472

473 **E3 ubiquitin ligase activity assay**

474 MBP- tagged fusion proteins were expressed in *E. coli* strain BL21 (DE3) and purified with
475 Amylose Resin (E8021S; NEB) by following the protocol provided by the manufacturer. The
476 purified proteins were further desalted and concentrated using the Amicon Centrifugal Filter
477 (Millipore). The concentration of purified protein was determined using protein assay agent
478 (Bio-Rad).

479

480 The *in vitro* ubiquitination assay was performed as described (Zhou et al., 2017). Briefly, the
481 components of 3 µg FLAG-ubiquitin, 40 ng E1 (GST-SIUBA1), 120 ng 6xHIS-AtUBC8 with 4
482 µg MBP, MBP-MAC3A, MBP-MAC3A^{Mut1}, or MBP-MAC3A^{Mut1} proteins were added to a 30
483 µL reaction buffer [50 mM Tris-HCl pH7.5, 5 mM ATP, 5 mM MgCl₂, 2 mM dithiothreitol
484 (DTT), 3 mM creatine phosphate, 5 µg/ml creatine phosphokinase]. To detect the influence of
485 protein modification on MAC3A activity, the recombinant proteins were treated as previously
486 described with modifications (Wang et al., 2015). Briefly, 4 µg MBP, MBP-MAC3A, MBP-
487 MAC3A^{Mut1}, or MBP-MAC3A^{Mut1}-bound amylose resin were incubated with the total protein
488 extracts from *mac3a mac3b* for one hour at room temperature followed by extensively washing
489 for three times. Following treatment, half of protein-bound resin was treated with calf intestinal
490 alkaline phosphatase (CIP; NEB) for 30 min, while the other half was incubated with reaction
491 buffer without CIP. After washing, protein-bounded resins were used to perform ubiquitin assay
492 as described above. The reaction was terminated by addition of SDS sample loading buffer with

493 100 mM DTT. FLAG-ubiquitin and MBP-MAC3A were then detected with a mouse monoclonal
494 anti-FLAG M2-peroxidase-conjugated antibody (A8592, Sigma-Aldrich) and anti-MBP antibody
495 (E8030, NEB), respectively.

496

497 **Co-IP Assay**

498 To test the interaction between MAC3A and RPB2, anti-RPB2 antibody was used to perform IP
499 on the protein extracts from inflorescences of transgenic plants harboring *pro35S:MAC3A-GFP*
500 (Ren et al., 2012). After IP, MAC3A-GFP and RPB2 were detected by immunoblot using an
501 anti-GFP monoclonal antibody (B230720, Biolegend) and anti-RPB2 antibodies (ab10338,
502 Abcam). To examine the co-IP of MAC3A with CDC5, and PRL1, MYC-MAC3A was co-
503 expressed with YFP, CDC5-YFP or PRL1-YFP in *N. benthamiana* as described (Ren et al.,
504 2012). To examine the co-IP of MAC3A with DCL1 and SE, MAC3A-YFP was co-expressed
505 with MYC-DCL1 or MYC-SE in *N. benthamiana*. IP was performed on protein extracts using
506 anti-GFP or anti-MYC antibodies coupled to protein G agarose beads as described (Ren et al.,
507 2012). After IP, proteins were detected with immunoblotting using monoclonal antibodies
508 against YFP (B230720, Biolegend) or MYC (06-340, Millipore).

509

510 **ChIP assay**

511 ChIP was performed using 14-d-old seedlings from Col-0 and *mac3a mac3b* as described (Kim
512 et al., 2011). Three biological replicates were performed. Anti-RPB2 antibody (ab10338, Abcam)
513 was used for immunoprecipitation. qPCR was performed using primers listed in Supplemental
514 Table 1.

515

516 **Dicer Activity Assay**

517 *In vitro* MIR162b processing assay was performed as described (Qi et al., 2005; Ren et al.,
518 2012). DNA templates used for *in vitro* transcription were generated through PCR with primers
519 listed in Supplemental Table 1. *In vitro* transcription of *MIR162b*, *N-UBQ5* and anti-sense *N-*
520 *UBQ5* were performed using T7 RNA polymerase in the presence of [α -³²P] UTP, ATP, CTP,
521 GTP and unlabeled UTP. *MIR162b* was processed in reaction buffer (100 mM NaCl, 1 mM ATP,
522 0.2 mM GTP, 1.2 mM MgCl₂, 25 mM creatine phosphate, 30 μ g/ml creatine kinase and 4 U

523 RNase inhibitor) containing 30 µg protein at 25 °C. After the reaction was stopped at 50 or 100
524 minutes, RNAs were extracted and separated on a PAGE gel. ImageQuant was used to quantify
525 the radioactive signals detected by a PhosphorImager.

526

527 **Morphological analyses and GUS histochemical staining**

528 Morphological and cellular analyses were performed according to the previously reported
529 methods (Li et al., 2012). GUS staining was performed as described (Zhang et al., 2013). Briefly,
530 tissues from plants of *mac3a mac3b* harboring *proMAC3A:MAC3A-GUS* or plants harboring
531 *proMIR167a:GUS* were incubated with staining solution at 37 °C for 5 hours. 70% ethanol was
532 used for tissue clearing before imaging.

533

534 **BiFC Assay**

535 BiFC assay was performed as described (Zhang et al., 2013). Paired cCFP and nVenus fusion
536 proteins were co-expressed in *N. benthamiana* leaves. After 40 h expression, a confocal
537 microscope (Fluoview 500 workstation; Olympus) was used to detect YFP and chlorophyll
538 autofluorescence signals at 488 nm with a narrow barrier (505–525 nm, BA505-525; Olympus).

539

540 **RNA gel blot and RT-qPCR analyses**

541 RNA gel blotting was performed as described (Ren et al., 2012). ~15 µg total RNAs extracted
542 from inflorescences were resolved on 16% PAGE gel and transferred to nylon membranes. ³²P-
543 labelled antisense DNA oligonucleotides were used to detect small RNAs. Radioactive signals
544 were detected with a Phosphorimager and quantified with ImageQuant. Inflorescences of plants
545 grown on three different growth rooms at the same condition (22°C with 16 hour light and 8 hour
546 dark cycles) were harvested as three replicates. The levels of pri-miRNAs, miRNA target
547 transcripts and GUS mRNA were determined using RT-qPCR. 1 µg total RNAs from
548 inflorescences were used to generate cDNAs using the SuperScript III reverse transcriptase
549 (Invitrogen) and an oligo dT18 primer. cDNAs were then used as templates for qPCR on an
550 iCycler apparatus (Bio-Rad) with the SYBR green kit (Bio-Rad). The primers used for PCR are
551 listed on Supplemental Table 1.

552

553 **RNA immunoprecipitation (RIP) analyses**

554 RIP was performed according to (Wierzbicki et al., 2008; Ren et al., 2012). ~ 2g seedlings of
555 transgenic plants harboring the *pro35S:MYC-MAC3A* transgene were used to examine the
556 association of MAC3A with pri-miRNAs *in vivo*. After crosslinking with 1% formaldehyde for
557 10 min, glycine was added to quench the reaction for 10 min. Nuclei were extracted and lysed in
558 the buffer (50 mM Tris-HCl, pH8.0, 10 mM EDTA, 1% SDS) by sonication for five times. After
559 debris was removed by centrifugation at 16,000g for 10 min, equal amounts of proteins from
560 various samples were diluted with RIP dilution buffer and incubated with anti-GFP antibodies
561 conjugated to protein-G agarose beads. The immunoprecipitates were then eluted with elution
562 buffer (100 mM NaHCO₃, 1% SDS) at 65 °C. Following reverse crosslinking with proteinase K
563 (Invitrogen) and 200 mM NaCl at 65 °C, RNAs were extracted and used as templates for RT-
564 PCR analyses. All the primers are listed in Supplemental Table 1.

565

566 ***In vitro* RNA pull-down assay**

567 *In vitro* RNA pull-down assay was performed as described (Ren et al., 2012). The amylose resin
568 beads containing MBP or MBP-MAC3A were incubated with [³²P]-labeled probes at 4°C for 1
569 hour. After the beads were washed for 4 times, RNAs were extracted and resolved on PAGE
570 gels. Radioactive signals were detected with a PhosphorImager and quantified by ImageQuant.

571

572 **Small RNA sequencing**

573 Inflorescences of Col, *mac3a mac3b* and *cdc5-1* grown on two separate growth rooms at the
574 same condition (22°C with 16 hour light and 8 hour dark cycles) were harvested as two
575 biological replicates and used for RNA extraction and small RNA library preparation following
576 standard protocol. The data set was deposited into the National Center for Biotechnology
577 Information Gene Expression Omnibus (Col accession #: GSM2829820, GSM2829821, *mac3a*
578 *mac3b* accession # GSM2829822, GSM2829823; Col accession #: GSM2805383, GSM2805384,
579 *cdc5-1* accession #: GSM2805385, GSM2805386). The sequencing data (Col access #:
580 GSM2257315, GSM2257316, GSM2257317; *dcl1* accession #: GSM2257321, GSM2257322,
581 GSM2257323) generated by Wu et al., (Wu et al., 2016) were used to analyze the effect of
582 DCL1 on miRNA accumulation. After sequencing, miRNA analysis was performed after
583 removing reads aligned to t/r/sn/snoRNA according to Ren et al (Ren et al., 2012).
584 Normalization was done using the total numbers of perfectly aligned reads (Nobuta et al., 2010).

585 The mean values of miRNA abundance from biological replicates were compared by using
586 EdgeR with trimmed mean of M values (TMM) normalization method (Robinson et al., 2010).
587 Down-regulated miRNAs with confidence ($P < 0.1$; $\text{fold} < 0.7$) were used to identify the
588 overlapping effect of *mac3a mac3b*, *cdc5-1* and *dcl1-9*. The Venn diagram was plotted with the
589 VennDiagram from the R package (Chen and Boutros, 2011).

590

591 Accession Numbers

592 Sequence data from this article can be found in the Arabidopsis Genome Initiative or
593 GenBank/EMBL databases under the following accession numbers: *MAC3A* (AT1G04510),
594 *MAC3B* (AT2G33340), *CDC5* (AT1G09770), *PRL1* (AT4G15900), *DCLI* (AT1G01040), *SE*
595 (AT2G27100), *HYL1* (AT1G09700), *DDL* (AT3G20550), *CBP20* (AT5G44200), *CBP80*
596 (AT2G13540), *HEN1* (AT4G20910), *AGO1* (AT1G48410), *ARF4* (AT5G60450), *ARF8*
597 (AT5G37020), *CKB3* (AT3G60250), *CUC1* (AT3G15170), *MYB33* (AT5G06100), *PHV*
598 (AT1G30490), *PHO2* (AT2G33770), *PPR* (AT1G62670), *SPL9* (AT2G42200), *SPL10*
599 (AT1G27370), *SPL13* (AT5G50570), *UBIQUITIN5* (AT3G62250). Protein sequences of MAC3
600 homologs in other species can be obtained in National Center for Biotechnology Information
601 under the following accession numbers: AAN13133 (*MAC3A*, AT1G04510, *Arabidopsis*
602 *thaliana*), FJ820118 (*MAC3B*, AT2G33340, *Arabidopsis thaliana*), XP_009143870 (*Brassica*
603 *rapa*), XP_009141306 (*Brassica rapa*), XP_004247768 (*Solanum lycopersicum*),
604 XP_003555746 (*Glycine max*), XP_003535988 (*Glycine max*), XP_015614850 (Os10g32880,
605 *Oryza sativa*), KXG38386 (SORBI_3001G226000, *Sorghum bicolor*), ONM06005
606 (ZEAMMB73_Zm00001d032763, *Zea mays*), AQK65171 (ZEAMMB73_Zm00001d014078,
607 *Zea mays*), XP_001701820 (*Chlamydomonas reinhardtii*), NP_055317 (HsPRP19, *Homo*
608 *sapiens*), NP_598890 (MmPRP19, *Mus musculus*), CAB10135 (SpPRP19, *Shizosaccharomyces*
609 *pombe*), and CAA97487 (ScPRP19, *Saccharomyces cerevisiae*). Small RNA deep sequencing
610 datasets are available from the National Center for Biotechnology Information Gene Expression
611 Omnibus under the following reference numbers: Col accession #: GSM2829820, GSM2829821,
612 *mac3a mac3b* accession # GSM2829822, GSM2829823; Col accession #: GSM2805383,
613 GSM2805384, *cdc5-1* accession #: GSM2805385, GSM2805386; Col access #: GSM2257315,
614 GSM2257316, GSM2257317; *dcl1* accession #: GSM2257321, GSM2257322, GSM2257323.

615

616 Supplemental Data

617 **Supplemental Figure 1.** Small RNA sequencing analyses of *mac3a mac3b*, *cdc5* and *dcl1-9*.
618 (Supports Figure 2)
619 **Supplemental Figure 2.** Expression of *MAC3A* and *MAC3B* complements the defects of *mac3a*
620 *mac3b*. (Supports Figure 2)
621 **Supplemental Figure 3.** Effect of *MAC3A* and *MAC3B* on the expression levels and splicing of
622 genes involved in miRNA biogenesis. (Supports Figure 4)
623 **Supplemental Figure 4.** Interaction of *MAC3B* with *CDC5*, *PRL1* and the *DCL1* complex
624 detected by BiFC analysis. (Supports Figure 4)
625 **Supplemental Figure 5.** RNA-binding activity of *MAC3A*. (Supports Figure 5)
626 **Supplemental Figure 6.** *HYL1-YFP* localization in root tips in *Col* and *mac3a mac3b* mutant.
627 (Supports Figure 6).
628 **Supplemental Figure 7.** Phylogenetic analysis of *MAC3A* orthologs. (Supports Figure 7)
629 **Supplemental Figure 8.** Ubiquitin ligase activity of *MAC3A* is required for miRNA
630 biogenesis. (Supports Figure 8)
631 **Supplemental Table 1.** The sequences of oligonucleotides.
632 **Supplemental Data Set 1.** miRNA profile change in *mac3a mac3b*, *cdc5-1*, and *dcl1-9* relative
633 to wild-type plants as determined by small RNA sequencing. (Supports Supplemental Figure 1)
634 **Supplemental Data Set 2.** Text file of the alignment used for the phylogenetic analysis shown in
635 Supplemental Figure 7. (Supports Figure 7)
636 **Supplemental Data Set 3.** Results of statistical analyses (Supports Figures 1, 2, 3, 5, 6, 8, and
637 Supplemental Figures 2, 3)

638

639 **Acknowledgements**

640 This work was supported by the Nebraska Soybean Board (Award #1727 to B.Y), the National
641 Science Foundation (Awards OIA- 1557417 to B.Y and IOS-1645659 to L.Z), and the Pioneer
642 Hundred Talents Program of Chinese Academy of Sciences (to S.L).

643

644 **Author Contributions**

645 S.L. and B.Y. designed the experiments and prepared the manuscript. S.L., B.Y., K.L., B.Z., M.L.,
646 S.Z., L.Z. and C.Z. performed the experiments. S.L., C.Z. and B.Y. analyzed the data.

647

648 **Competing Financial Interests**

649 The authors declare no competing financial interests.

650

651

Parsed Citations

Allen, E., Xie, Z., Gustafson, A.M., and Carrington, J.C. (2005). microRNA-directed phasing during trans-acting siRNA biogenesis in plants. *Cell* 121, 207-221.

Pubmed: [Author and Title](#)

CrossRef: [Author and Title](#)

Google Scholar: [Author Only](#) [Title Only](#) [Author and Title](#)

Axtell, M.J. (2013). Classification and comparison of small RNAs from plants. *Annu Rev Plant Biol* 64, 137-159.

Pubmed: [Author and Title](#)

CrossRef: [Author and Title](#)

Google Scholar: [Author Only](#) [Title Only](#) [Author and Title](#)

Axtell, M.J., Jan, C., Rajagopalan, R., and Bartel, D.P. (2006). A two-hit trigger for siRNA biogenesis in plants. *Cell* 127, 565-577.

Pubmed: [Author and Title](#)

CrossRef: [Author and Title](#)

Google Scholar: [Author Only](#) [Title Only](#) [Author and Title](#)

Baulcombe, D. (2004). RNA silencing in plants. *Nature* 431, 356-363.

Pubmed: [Author and Title](#)

CrossRef: [Author and Title](#)

Google Scholar: [Author Only](#) [Title Only](#) [Author and Title](#)

Baumberger, N., and Baulcombe, D.C. (2005). Arabidopsis ARGONAUTE1 is an RNA Slicer that selectively recruits microRNAs and short interfering RNAs. *Proc Natl Acad Sci U S A* 102, 11928-11933.

Pubmed: [Author and Title](#)

CrossRef: [Author and Title](#)

Google Scholar: [Author Only](#) [Title Only](#) [Author and Title](#)

Ben Chaabane, S., Liu, R., Chinnusamy, V., Kwon, Y., Park, J.H., Kim, S.Y., Zhu, J.K., Yang, S.W., and Lee, B.H. (2013). STA1, an Arabidopsis pre-mRNA processing factor 6 homolog, is a new player involved in miRNA biogenesis. *Nucleic Acids Res* 41, 1984-1997.

Pubmed: [Author and Title](#)

CrossRef: [Author and Title](#)

Google Scholar: [Author Only](#) [Title Only](#) [Author and Title](#)

Bologna, N.G., Schapire, A.L., Zhai, J., Chorostecki, U., Boisbouvier, J., Meyers, B.C., and Palatnik, J.F. (2013). Multiple RNA recognition patterns during microRNA biogenesis in plants. *Genome research* 23, 1675-1689.

Pubmed: [Author and Title](#)

CrossRef: [Author and Title](#)

Google Scholar: [Author Only](#) [Title Only](#) [Author and Title](#)

Chanarat, S., and Strasser, K. (2013). Splicing and beyond: the many faces of the Prp19 complex. *Biochim Biophys Acta* 1833, 2126-2134.

Pubmed: [Author and Title](#)

CrossRef: [Author and Title](#)

Google Scholar: [Author Only](#) [Title Only](#) [Author and Title](#)

Chen, H., and Boutros, P.C. (2011). VennDiagram: a package for the generation of highly-customizable Venn and Euler diagrams in R. *BMC Bioinformatics* 12, 35.

Pubmed: [Author and Title](#)

CrossRef: [Author and Title](#)

Google Scholar: [Author Only](#) [Title Only](#) [Author and Title](#)

Chen, T., Cui, P., and Xiong, L. (2015). The RNA-binding protein HOS5 and serine/arginine-rich proteins RS40 and RS41 participate in miRNA biogenesis in Arabidopsis. *Nucleic Acids Res* 43, 8283-8298.

Pubmed: [Author and Title](#)

CrossRef: [Author and Title](#)

Google Scholar: [Author Only](#) [Title Only](#) [Author and Title](#)

Cho, S.K., Ben Chaabane, S., Shah, P., Poulsen, C.P., and Yang, S.W. (2014). COP1 E3 ligase protects HYL1 to retain microRNA biogenesis. *Nature communications* 5, 5867.

Pubmed: [Author and Title](#)

CrossRef: [Author and Title](#)

Google Scholar: [Author Only](#) [Title Only](#) [Author and Title](#)

Das, T., Park, J.K., Park, J., Kim, E., Rape, M., Kim, E.E., and Song, E.J. (2017). USP15 regulates dynamic protein-protein interactions of the spliceosome through deubiquitination of PRP31. *Nucleic Acids Res*.

Pubmed: [Author and Title](#)

CrossRef: [Author and Title](#)

Google Scholar: [Author Only](#) [Title Only](#) [Author and Title](#)

Deng, X., Lu, T., Wang, L., Gu, L., Sun, J., Kong, X., Liu, C., and Cao, X. (2016). Recruitment of the NineTeen Complex to the activated spliceosome requires AtPRMT5. *Proc Natl Acad Sci U S A* 113, 5447-5452.

Pubmed: [Author and Title](#)

CrossRef: [Author and Title](#)

Google Scholar: [Author Only](#) [Title Only](#) [Author and Title](#)

Dong, Z., Han, M.H., and Fedoroff, N. (2008). The RNA-binding proteins HYL1 and SE promote accurate in vitro processing of pri-miRNA by DCL1. *Proc Natl Acad Sci U S A* 105, 9970-9975.

Pubmed: [Author and Title](#)

CrossRef: [Author and Title](#)

Google Scholar: [Author Only](#) [Title Only](#) [Author and Title](#)

Earley, K.W., and Poethig, R.S. (2011). Binding of the cyclophilin 40 ortholog SQUINT to Hsp90 protein is required for SQUINT function in *Arabidopsis*. *J Biol Chem* 286, 38184-38189.

Pubmed: [Author and Title](#)

CrossRef: [Author and Title](#)

Google Scholar: [Author Only](#) [Title Only](#) [Author and Title](#)

Fang, X., Cui, Y., Li, Y., and Qi, Y. (2015a). Transcription and processing of primary microRNAs are coupled by Elongator complex in *Arabidopsis*. *Nat Plants* 1, 15075.

Pubmed: [Author and Title](#)

CrossRef: [Author and Title](#)

Google Scholar: [Author Only](#) [Title Only](#) [Author and Title](#)

Fang, X., Shi, Y., Liu, X., Chen, Z., and Qi, Y. (2015b). CMA33/XCT Regulates Small RNA Production through Modulating the Transcription of Dicer-Like Genes in *Arabidopsis*. *Mol Plant*.

Pubmed: [Author and Title](#)

CrossRef: [Author and Title](#)

Google Scholar: [Author Only](#) [Title Only](#) [Author and Title](#)

Fang, Y., and Spector, D.L. (2007). Identification of nuclear dicing bodies containing proteins for microRNA biogenesis in living *Arabidopsis* plants. *Curr Biol* 17, 818-823.

Pubmed: [Author and Title](#)

CrossRef: [Author and Title](#)

Google Scholar: [Author Only](#) [Title Only](#) [Author and Title](#)

Francisco-Mangilet, A.G., Karlsson, P., Kim, M.H., Eo, H.J., Oh, S.A., Kim, J.H., Kulcheski, F.R., Park, S.K., and Manavella, P.A. (2015). THO2, a core member of the THO/TREX complex, is required for microRNA production in *Arabidopsis*. *Plant J* 82, 1018-1029.

Pubmed: [Author and Title](#)

CrossRef: [Author and Title](#)

Google Scholar: [Author Only](#) [Title Only](#) [Author and Title](#)

Fujioka, Y., Utsumi, M., Ohba, Y., and Watanabe, Y. (2007). Location of a possible miRNA processing site in SmD3/SmB nuclear bodies in *Arabidopsis*. *Plant Cell Physiol* 48, 1243-1253.

Pubmed: [Author and Title](#)

CrossRef: [Author and Title](#)

Google Scholar: [Author Only](#) [Title Only](#) [Author and Title](#)

Gregory, B.D., O'Malley, R.C., Lister, R., Urich, M.A., Tonti-Filippini, J., Chen, H., Millar, A.H., and Ecker, J.R. (2008). A link between RNA metabolism and silencing affecting *Arabidopsis* development. *Dev Cell* 14, 854-866.

Pubmed: [Author and Title](#)

CrossRef: [Author and Title](#)

Google Scholar: [Author Only](#) [Title Only](#) [Author and Title](#)

Hajheidari, M., Farrona, S., Huettel, B., Koncz, Z., and Koncz, C. (2012). CDKF;1 and CDKD protein kinases regulate phosphorylation of serine residues in the C-terminal domain of *Arabidopsis* RNA polymerase II. *Plant Cell* 24, 1626-1642.

Pubmed: [Author and Title](#)

CrossRef: [Author and Title](#)

Google Scholar: [Author Only](#) [Title Only](#) [Author and Title](#)

Karlsson, P., Christie, M.D., Seymour, D.K., Wang, H., Wang, X., Hagemann, J., Kulcheski, F., and Manavella, P.A. (2015). KH domain protein RCF3 is a tissue-biased regulator of the plant miRNA biogenesis cofactor HYL1. *Proc Natl Acad Sci U S A* 112, 14096-14101.

Pubmed: [Author and Title](#)

CrossRef: [Author and Title](#)

Google Scholar: [Author Only](#) [Title Only](#) [Author and Title](#)

Kim, W., Benhamed, M., Servet, C., Latrassé, D., Zhang, W., Delarue, M., and Zhou, D.X. (2009). Histone acetyltransferase GCN5 interferes with the miRNA pathway in *Arabidopsis*. *Cell research* 19, 899-909.

Pubmed: [Author and Title](#)

CrossRef: [Author and Title](#)

Google Scholar: [Author Only](#) [Title Only](#) [Author and Title](#)

Kim, Y.J., Zheng, B., Yu, Y., Won, S.Y., Mo, B., and Chen, X. (2011). The role of Mediator in small and long noncoding RNA production in *Arabidopsis thaliana*. *EMBO J* 30, 814-822.

Pubmed: [Author and Title](#)

CrossRef: [Author and Title](#)

Google Scholar: [Author Only](#) [Title Only](#) [Author and Title](#)

Koster, T., Meyer, K., Weinholdt, C., Smith, L.M., Lummer, M., Speth, C., Grosse, I., Weigel, D., and Staiger, D. (2014). Regulation of pri-miRNA processing by the hnRNP-like protein AtGRP7 in *Arabidopsis*. *Nucleic Acids Res* 42, 9925-9936.

- Pubmed: [Author and Title](#)
CrossRef: [Author and Title](#)
Google Scholar: [Author Only Title Only Author and Title](#)
- Lau, C.K., Bachorik, J.L., and Dreyfuss, G. (2009).** Gemin5-snRNA interaction reveals an RNA binding function for WD repeat domains. *Nat Struct Mol Biol* 16, 486-491.
- Pubmed: [Author and Title](#)
CrossRef: [Author and Title](#)
Google Scholar: [Author Only Title Only Author and Title](#)
- Laubinger, S., Sachsenberg, T., Zeller, G., Busch, W., Lohmann, J.U., Ratsch, G., and Weigel, D. (2008).** Dual roles of the nuclear cap-binding complex and SERRATE in pre-mRNA splicing and microRNA processing in *Arabidopsis thaliana*. *Proc Natl Acad Sci U S A* 105, 8795-8800.
- Pubmed: [Author and Title](#)
CrossRef: [Author and Title](#)
Google Scholar: [Author Only Title Only Author and Title](#)
- Li, S., Liu, K., Zhang, S., Wang, X., Rogers, K., Ren, G., Zhang, C., and Yu, B. (2017).** STV1, a ribosomal protein, binds primary microRNA transcripts to promote their interaction with the processing complex in *Arabidopsis*. *Proc Natl Acad Sci U S A* 114, 1424-1429.
- Pubmed: [Author and Title](#)
CrossRef: [Author and Title](#)
Google Scholar: [Author Only Title Only Author and Title](#)
- Li, S., Liu, Y., Zheng, L., Chen, L., Li, N., Corke, F., Lu, Y., Fu, X., Zhu, Z., Bevan, M.W., and Li, Y. (2012).** The plant-specific G protein gamma subunit AGG3 influences organ size and shape in *Arabidopsis thaliana*. *New Phytol* 194, 690-703.
- Pubmed: [Author and Title](#)
CrossRef: [Author and Title](#)
Google Scholar: [Author Only Title Only Author and Title](#)
- Manavella, P.A., Hagmann, J., Ott, F., Laubinger, S., Franz, M., Macek, B., and Weigel, D. (2012).** Fast-forward genetics identifies plant CPL phosphatases as regulators of miRNA processing factor HYL1. *Cell* 151, 859-870.
- Pubmed: [Author and Title](#)
CrossRef: [Author and Title](#)
Google Scholar: [Author Only Title Only Author and Title](#)
- Marechal, A., Li, J.M., Ji, X.Y., Wu, C.S., Yazinski, S.A., Nguyen, H.D., Liu, S., Jimenez, A.E., Jin, J., and Zou, L. (2014).** PRP19 transforms into a sensor of RPA-ssDNA after DNA damage and drives ATR activation via a ubiquitin-mediated circuitry. *Molecular cell* 53, 235-246.
- Pubmed: [Author and Title](#)
CrossRef: [Author and Title](#)
Google Scholar: [Author Only Title Only Author and Title](#)
- Mateos, J.L., Bologna, N.G., Chorostecki, U., and Palatnik, J.F. (2010).** Identification of microRNA processing determinants by random mutagenesis of *Arabidopsis* MIR172a precursor. *Curr Biol* 20, 49-54.
- Pubmed: [Author and Title](#)
CrossRef: [Author and Title](#)
Google Scholar: [Author Only Title Only Author and Title](#)
- McGrail, J.C., Krause, A., and O'Keefe, R.T. (2009).** The RNA binding protein Cwc2 interacts directly with the U6 snRNA to link the nineteen complex to the spliceosome during pre-mRNA splicing. *Nucleic Acids Res* 37, 4205-4217.
- Pubmed: [Author and Title](#)
CrossRef: [Author and Title](#)
Google Scholar: [Author Only Title Only Author and Title](#)
- Monaghan, J., Xu, F., Xu, S., Zhang, Y., and Li, X. (2010).** Two putative RNA-binding proteins function with unequal genetic redundancy in the MOS4-associated complex. *Plant Physiol* 154, 1783-1793.
- Pubmed: [Author and Title](#)
CrossRef: [Author and Title](#)
Google Scholar: [Author Only Title Only Author and Title](#)
- Monaghan, J., Xu, F., Gao, M., Zhao, Q., Palma, K., Long, C., Chen, S., Zhang, Y., and Li, X. (2009).** Two Prp19-like U-box proteins in the MOS4-associated complex play redundant roles in plant innate immunity. *PLoS Pathog* 5, e1000526.
- Pubmed: [Author and Title](#)
CrossRef: [Author and Title](#)
Google Scholar: [Author Only Title Only Author and Title](#)
- Nobuta, K., McCormick, K., Nakano, M., and Meyers, B.C. (2010).** Bioinformatics analysis of small RNAs in plants using next generation sequencing technologies. *Methods Mol Biol* 592, 89-106.
- Pubmed: [Author and Title](#)
CrossRef: [Author and Title](#)
Google Scholar: [Author Only Title Only Author and Title](#)
- Ohi, M.D., Vander Kooi, C.W., Rosenberg, J.A., Chazin, W.J., and Gould, K.L. (2003).** Structural insights into the U-box, a domain associated with multi-ubiquitination. *Nat Struct Biol* 10, 250-255.
- Pubmed: [Author and Title](#)
CrossRef: [Author and Title](#)
Google Scholar: [Author Only Title Only Author and Title](#)

Palma, K., Zhao, Q., Cheng, Y.T., Bi, D., Monaghan, J., Cheng, W., Zhang, Y., and Li, X. (2007). Regulation of plant innate immunity by three proteins in a complex conserved across the plant and animal kingdoms. *Genes Dev* 21, 1484-1493.

Pubmed: [Author and Title](#)

CrossRef: [Author and Title](#)

Google Scholar: [Author Only](#) [Title Only](#) [Author and Title](#)

Peragine, A., Yoshikawa, M., Wu, G., Albrecht, H.L., and Poethig, R.S. (2004). SGS3 and SGS2/SDE1/RDR6 are required for juvenile development and the production of trans-acting siRNAs in Arabidopsis. *Genes Dev* 18, 2368-2379.

Pubmed: [Author and Title](#)

CrossRef: [Author and Title](#)

Google Scholar: [Author Only](#) [Title Only](#) [Author and Title](#)

Qi, Y., Denli, A.M., and Hannon, G.J. (2005). Biochemical specialization within Arabidopsis RNA silencing pathways. *Molecular cell* 19, 421-428.

Pubmed: [Author and Title](#)

CrossRef: [Author and Title](#)

Google Scholar: [Author Only](#) [Title Only](#) [Author and Title](#)

Qiao, Y., Shi, J., Zhai, Y., Hou, Y., and Ma, W. (2015). Phytophthora effector targets a novel component of small RNA pathway in plants to promote infection. *Proc Natl Acad Sci U S A* 112, 5850-5855.

Pubmed: [Author and Title](#)

CrossRef: [Author and Title](#)

Google Scholar: [Author Only](#) [Title Only](#) [Author and Title](#)

Ren, G., Chen, X., and Yu, B. (2014). Small RNAs meet their targets: when methylation defends miRNAs from uridylation. *RNA Biol* 11, 1099-1104.

Pubmed: [Author and Title](#)

CrossRef: [Author and Title](#)

Google Scholar: [Author Only](#) [Title Only](#) [Author and Title](#)

Ren, G., Xie, M., Dou, Y., Zhang, S., Zhang, C., and Yu, B. (2012). Regulation of miRNA abundance by RNA binding protein TOUGH in Arabidopsis. *Proc Natl Acad Sci U S A* 109, 12817-12821.

Pubmed: [Author and Title](#)

CrossRef: [Author and Title](#)

Google Scholar: [Author Only](#) [Title Only](#) [Author and Title](#)

Robinson, M.D., McCarthy, D.J., and Smyth, G.K. (2010). edgeR: a Bioconductor package for differential expression analysis of digital gene expression data. *Bioinformatics* 26, 139-140.

Pubmed: [Author and Title](#)

CrossRef: [Author and Title](#)

Google Scholar: [Author Only](#) [Title Only](#) [Author and Title](#)

Smith, M.R., Willmann, M.R., Wu, G., Berardini, T.Z., Moller, B., Weijers, D., and Poethig, R.S. (2009). Cyclophilin 40 is required for microRNA activity in Arabidopsis. *Proc Natl Acad Sci U S A* 106, 5424-5429.

Pubmed: [Author and Title](#)

CrossRef: [Author and Title](#)

Google Scholar: [Author Only](#) [Title Only](#) [Author and Title](#)

Song, L., Axtell, M.J., and Fedoroff, N.V. (2010). RNA secondary structural determinants of miRNA precursor processing in Arabidopsis. *Curr Biol* 20, 37-41.

Pubmed: [Author and Title](#)

CrossRef: [Author and Title](#)

Google Scholar: [Author Only](#) [Title Only](#) [Author and Title](#)

Song, L., Han, M.H., Lesicka, J., and Fedoroff, N. (2007). Arabidopsis primary microRNA processing proteins HYL1 and DCL1 define a nuclear body distinct from the Cajal body. *Proc Natl Acad Sci U S A* 104, 5437-5442.

Pubmed: [Author and Title](#)

CrossRef: [Author and Title](#)

Google Scholar: [Author Only](#) [Title Only](#) [Author and Title](#)

Speth, C., Willing, E.M., Rausch, S., Schneeberger, K., and Laubinger, S. (2013). RACK1 scaffold proteins influence miRNA abundance in Arabidopsis. *Plant J* 76, 433-445.

Pubmed: [Author and Title](#)

CrossRef: [Author and Title](#)

Google Scholar: [Author Only](#) [Title Only](#) [Author and Title](#)

Vander Kooi, C.W., Ren, L., Xu, P., Ohi, M.D., Gould, K.L., and Chazin, W.J. (2010). The Prp19 WD40 domain contains a conserved protein interaction region essential for its function. *Structure* 18, 584-593.

Pubmed: [Author and Title](#)

CrossRef: [Author and Title](#)

Google Scholar: [Author Only](#) [Title Only](#) [Author and Title](#)

Vaucheret, H. (2008). Plant ARGONAUTES. *Trends Plant Sci* 13, 350-358.

Pubmed: [Author and Title](#)

- CrossRef: [Author and Title](#)
Google Scholar: [Author Only Title Only Author and Title](#)
- Voinnet, O. (2009).** Origin, biogenesis, and activity of plant microRNAs. *Cell* 136, 669-687.
Pubmed: [Author and Title](#)
CrossRef: [Author and Title](#)
Google Scholar: [Author Only Title Only Author and Title](#)
- Wang, J., Qu, B., Dou, S., Li, L., Yin, D., Pang, Z., Zhou, Z., Tian, M., Liu, G., Xie, Q., Tang, D., Chen, X., and Zhu, L. (2015).** The E3 ligase OsPUB15 interacts with the receptor-like kinase PID2 and regulates plant cell death and innate immunity. *BMC plant biology* 15, 49.
Pubmed: [Author and Title](#)
CrossRef: [Author and Title](#)
Google Scholar: [Author Only Title Only Author and Title](#)
- Wang, L., Song, X., Gu, L., Li, X., Cao, S., Chu, C., Cui, X., Chen, X., and Cao, X. (2013).** NOT2 proteins promote polymerase II-dependent transcription and interact with multiple MicroRNA biogenesis factors in *Arabidopsis*. *Plant Cell* 25, 715-727.
Pubmed: [Author and Title](#)
CrossRef: [Author and Title](#)
Google Scholar: [Author Only Title Only Author and Title](#)
- Werner, S., Wollmann, H., Schneeberger, K., and Weigel, D. (2010).** Structure determinants for accurate processing of miR172a in *Arabidopsis thaliana*. *Curr Biol* 20, 42-48.
Pubmed: [Author and Title](#)
CrossRef: [Author and Title](#)
Google Scholar: [Author Only Title Only Author and Title](#)
- Wiborg, J., O'Shea, C., and Skriver, K. (2008).** Biochemical function of typical and variant *Arabidopsis thaliana* U-box E3 ubiquitin-protein ligases. *Biochem J* 413, 447-457.
Pubmed: [Author and Title](#)
CrossRef: [Author and Title](#)
Google Scholar: [Author Only Title Only Author and Title](#)
- Wierzbicki, A.T., Haag, J.R., and Pikaard, C.S. (2008).** Noncoding transcription by RNA polymerase Pol IVb/Pol V mediates transcriptional silencing of overlapping and adjacent genes. *Cell* 135, 635-648.
Pubmed: [Author and Title](#)
CrossRef: [Author and Title](#)
Google Scholar: [Author Only Title Only Author and Title](#)
- Wu, C., Li, X., Guo, S., and Wong, S.M. (2016).** Analyses of RNA-Seq and sRNA-Seq data reveal a complex network of anti-viral defense in TCV-infected *Arabidopsis thaliana*. *Sci Rep* 6, 36007.
Pubmed: [Author and Title](#)
CrossRef: [Author and Title](#)
Google Scholar: [Author Only Title Only Author and Title](#)
- Wu, X., Shi, Y., Li, J., Xu, L., Fang, Y., Li, X., and Qi, Y. (2013).** A role for the RNA-binding protein MOS2 in microRNA maturation in *Arabidopsis*. *Cell Res* 23, 645-657.
Pubmed: [Author and Title](#)
CrossRef: [Author and Title](#)
Google Scholar: [Author Only Title Only Author and Title](#)
- Xie, Z.X., Allen, E., Fahlgren, N., Calamar, A., Givan, S.A., and Carrington, J.C. (2005).** Expression of *Arabidopsis* MIRNA genes. *Plant Physiology* 138, 2145-2154.
Pubmed: [Author and Title](#)
CrossRef: [Author and Title](#)
Google Scholar: [Author Only Title Only Author and Title](#)
- Xu, F., Xu, S., Wiermer, M., Zhang, Y., and Li, X. (2012).** The cyclin L homolog MOS12 and the MOS4-associated complex are required for the proper splicing of plant resistance genes. *Plant J* 70, 916-928.
Pubmed: [Author and Title](#)
CrossRef: [Author and Title](#)
Google Scholar: [Author Only Title Only Author and Title](#)
- Yan, J., Wang, P., Wang, B., Hsu, C.C., Tang, K., Zhang, H., Hou, Y.J., Zhao, Y., Wang, Q., Zhao, C., Zhu, X., Tao, W.A., Li, J., and Zhu, J.K. (2017).** The SnRK2 kinases modulate miRNA accumulation in *Arabidopsis*. *PLoS genetics* 13, e1006753.
Pubmed: [Author and Title](#)
CrossRef: [Author and Title](#)
Google Scholar: [Author Only Title Only Author and Title](#)
- Yoshikawa, M., Peragine, A., Park, M.Y., and Poethig, R.S. (2005).** A pathway for the biogenesis of trans-acting siRNAs in *Arabidopsis*. *Genes Dev* 19, 2164-2175.
Pubmed: [Author and Title](#)
CrossRef: [Author and Title](#)
Google Scholar: [Author Only Title Only Author and Title](#)
- Yu, B., Bi, L., Zheng, B.L., Ji, L.J., Chevalier, D., Agarwal, M., Ramachandran, V., Li, W.X., Lagrange, T., Walker, J.C., and Chen, X.M. (2008).** The FHA domain proteins DAWDLE in *Arabidopsis* and SNIP1 in humans act in small RNA biogenesis. *Proc Natl Acad Sci U S A*

105, 10073-10078.

Pubmed: [Author and Title](#)

CrossRef: [Author and Title](#)

Google Scholar: [Author Only](#) [Title Only](#) [Author and Title](#)

Zhai, J., Zhao, Y., Simon, S.A., Huang, S., Petsch, K., Arikiti, S., Pillay, M., Ji, L., Xie, M., Cao, X., Yu, B., Timmermans, M., Yang, B., Chen, X., and Meyers, B.C. (2013). Plant MicroRNAs Display Differential 3'- Truncation and Tailing, Modifications Which Are ARGONAUTE1-Dependent and Conserved Across Species. *Plant Cell* 25, 2417-2428.

Pubmed: [Author and Title](#)

CrossRef: [Author and Title](#)

Google Scholar: [Author Only](#) [Title Only](#) [Author and Title](#)

Zhan, X., Wang, B., Li, H., Liu, R., Kalia, R.K., Zhu, J.K., and Chinnusamy, V. (2012). Arabidopsis proline-rich protein important for development and abiotic stress tolerance is involved in microRNA biogenesis. *Proc Natl Acad Sci U S A* 109, 18198-18203.

Pubmed: [Author and Title](#)

CrossRef: [Author and Title](#)

Google Scholar: [Author Only](#) [Title Only](#) [Author and Title](#)

Zhang, S., Liu, Y., and Yu, B. (2014). PRL1, an RNA-binding protein, positively regulates the accumulation of miRNAs and siRNAs in Arabidopsis. *PLoS genetics* 10, e1004841.

Pubmed: [Author and Title](#)

CrossRef: [Author and Title](#)

Google Scholar: [Author Only](#) [Title Only](#) [Author and Title](#)

Zhang, S., Liu, Y., and Yu, B. (2015). New insights into pri-miRNA processing and accumulation in plants. *Wiley Interdiscip Rev RNA* 6, 533-545.

Pubmed: [Author and Title](#)

CrossRef: [Author and Title](#)

Google Scholar: [Author Only](#) [Title Only](#) [Author and Title](#)

Zhang, S., Xie, M., Ren, G., and Yu, B. (2013). CDC5, a DNA binding protein, positively regulates posttranscriptional processing and/or transcription of primary microRNA transcripts. *Proc Natl Acad Sci U S A* 110, 17588-17593.

Pubmed: [Author and Title](#)

CrossRef: [Author and Title](#)

Google Scholar: [Author Only](#) [Title Only](#) [Author and Title](#)

Zhang, Z., Guo, X., Ge, C., Ma, Z., Jiang, M., Li, T., Koiwa, H., Yang, S.W., and Zhang, X. (2017). KETCH1 imports HYL1 to nucleus for miRNA biogenesis in Arabidopsis. *Proc Natl Acad Sci U S A* 114, 4011-4016.

Pubmed: [Author and Title](#)

CrossRef: [Author and Title](#)

Google Scholar: [Author Only](#) [Title Only](#) [Author and Title](#)

Zhou, B., Mural, R.V., Chen, X., Oates, M.E., Connor, R.A., Martin, G.B., Gough, J., and Zeng, L. (2017). A Subset of Ubiquitin-Conjugating Enzymes Is Essential for Plant Immunity. *Plant Physiol* 173, 1371-1390.

Pubmed: [Author and Title](#)

CrossRef: [Author and Title](#)

Google Scholar: [Author Only](#) [Title Only](#) [Author and Title](#)

Zhu, H., Zhou, Y., Castillo-Gonzalez, C., Lu, A., Ge, C., Zhao, Y.T., Duan, L., Li, Z., Axtell, M.J., Wang, X.J., and Zhang, X. (2013). Bidirectional processing of pri-miRNAs with branched terminal loops by Arabidopsis Dicer-like1. *Nat Struct Mol Biol* 20, 1106-1115.

Pubmed: [Author and Title](#)

CrossRef: [Author and Title](#)

Google Scholar: [Author Only](#) [Title Only](#) [Author and Title](#)

MAC3A and MAC3B, Two Core Subunits of the MOS4-Associated Complex, Positively Influence miRNA Biogenesis

Shengjun li, Kan Liu, Bangjun Zhou, Mu Li, Shuxin Zhang, Lirong Zeng, Chi Zhang and Bin Yu
Plant Cell; originally published online February 5, 2018;
DOI 10.1105/tpc.17.00953

This information is current as of February 8, 2018

Supplemental Data	/content/suppl/2018/02/05/tpc.17.00953.DC1.html
Permissions	https://www.copyright.com/ccc/openurl.do?sid=pd_hw1532298X&issn=1532298X&WT.mc_id=pd_hw1532298X
eTOCs	Sign up for eTOCs at: http://www.plantcell.org/cgi/alerts/ctmain
CiteTrack Alerts	Sign up for CiteTrack Alerts at: http://www.plantcell.org/cgi/alerts/ctmain
Subscription Information	Subscription Information for <i>The Plant Cell</i> and <i>Plant Physiology</i> is available at: http://www.aspb.org/publications/subscriptions.cfm